Solanum Incanum(L) Essential Oil Mediated Synthesis and Characterization of Fe_3O_4@Ag Nanocomposite for Methylene Blue Removal and Antibacterial Application

By: Yohannis Alemayehu

A Thesis Submitted to

The Department of Applied chemistry

School of Applied Natural Science.

Presented in Partial Fulfillment of the Requirement for the Degree of Masters in Chemistry (Industrial Stream)

Office of Graduate Studies

Adama Science and Technology University

July, 2020

Adama Ethiopia

Solanum Incanum(L) Essential Oil Mediated Synthesis and Characterization of Fe_3O_4@Ag Nanocomposite for Methylene Blue Removal and Antibacterial Application

By: Yohannis Alemayehu

Advisor: Dr. Aschalew Tadesse

Co-advisor: Dr. Teshome Abdo

A Thesis Submitted to

The Department of Applied chemistry

School of Applied Natural Science.

Presented in Partial Fulfillment of the Requirement for the Degree of Masters in Chemistry (Industrial Stream)

Office of Graduate Studies

Adama Science and Technology University

July, 2020

Adama, Ethiopia

Advisors Approval Sheet

To: Applied Chemistry Department

Subject: Thesis Submission

This is to certify that the thesis entitled "*Solanum Incanum(L)* Essential Oil Mediated Preparation and Characterization of Fe_3O_4@Ag Nanocomposite for Methylene Blue Removal and Antibacterial Application" submitted in partial fulfillment of the requirements for the degree of Masters in Chemistry (Industrial Stream) to the department of applied chemistry has been carried out by Yohannis Alemayehu Id. No PGR/18251/11 under our supervision. Therefore, we recommend that the student has fulfilled the requirements and hence hereby he can submit the thesis to the department.

Dr. Aschalew Tadesse	---	---
Advisor	Signature	Date
Dr. Teshome Abdo	---	---
Co-advisor	Signature	Date

Declaration

I hereby declare that this M.Sc. Thesis is my original work and has not been presented for a degree in any other university, and all source of materials used for this thesis have been duly acknowledged.

Yohannis Alemayehu

---------- ---------- ----------

Student Name Signature Date

This MSc Thesis has been submitted for examination with our approval as thesis advisors

Dr. Aschalew Tadesse

---------- ---------- ----------

Advisor Name Signature Date

Dr. Teshome Abdo

---------- ---------- ----------

Co-advisor Name Signature Date

Approval of Board of Examiners

We, the undersigned, members of the board of examiners of the final open defense by Yohannis Alemayehu have read and evaluated his thesis entitled *Solanum Incanum(L)* Essential Oil Mediated Preparation and Characterization of Fe_3O_4@Ag Nanocomposite for methylene blue removal and Antibacterial Application. This is, therefore, to certify that the thesis has been accepted in partial fulfillment of the requirement of the Degree of Masters.

Student	Yohannis Alemayehu	---------- Signature	---------- Date
Advisor	Dr. Aschalew Tadesse	---------- Signature	---------- Date
Co-Advisor	Dr. Teshome Abdo	---------- Signature	---------- Date
Chairperson	Dr. Fedlu Kedir	---------- Signature	---------- Date
External Examiner	----------	---------- Signature	---------- Date
Internal Examiner	----------	---------- Signature	---------- Date

ACKNOWLEDGMENT

First I would like to thank the only almighty God, who provides health, strength and accurate insight into reality for his divine intervention during my research work. Although this thesis work ultimately represents my accomplishments, I have benefited significantly from multiple peoples that I would like to acknowledge. First and foremost, I am grateful and thankful to my advisors, Dr. Aschalew Tadesse for his excellent supervision and scientific input in this research work. I would like to acknowledge Dr. Teshome Abdo for his contribution to this thesis work. I also thank greatly Dr Gemechu Deressa for his help in getting characterization techniques to characterize my sample (XRD, EDX, FTIR, TEM, SEM) in Korea.

I would like to express my sincere gratitude to all academic, technical and support staff of the department of Applied Chemistry, Adama Science and Technology University for providing the necessary knowledge, assistance and facilities to conduct my research work. Last but not least, I want to thank my family who were big sources of inspirations throughout my academic career with their valuable moral support and advice.

Acronyms and Abbreviation

EDX	Energy Dispersive X-Ray
EO	Essential Oil
Fig	Figure
FTIR	Fourier Transform Infrared spectroscopy
GC-MS	Gas Chromatography-Mass Spectrometry
NIST	National Institute of Standards and Technology
NPs	Nanoparticles
NC	Nanocomposite
MB	Methylene blue
SEM	Scanning Electron Microscope
TEM	Transmission Electron Microscope
UV-VIS	Ultraviolet Visible Spectroscopy
XRD	X-Ray Diffraction
TGA	Thermogravimetric Analysis
XPS	X-ray Photoelectron Spectroscopy (XPS)

Table of Contents

Contents **Page**

List of Figure

List of Tables

Abstract

In this study, Solanum Incanum (L) Essential Oil mediated silver nanoparticles (Ag NPs), magnetite nanoparticles (Fe_3O_4 NPs) and magnetite with silver nanocomposite (Fe_3O_4@Ag NC) preparation were described. There are three methods to synthesize nanoparticles physical, chemical and physical method. Biological is chosen because inexpensive, fast ecofriendly and nontoxic. Fe_3O_4 NPs, Ag NPs and Fe_3O_4@Ag NC prepared were characterized using field emission scanning electron microscopy (FESEM), Transmission electron microscopy (TEM), X-ray diffraction (XRD), Fourier-transform infrared (FTIR) spectroscopy and Ultraviolet-visible (UV-Vis) spectrophotometer. XRD results show that Ag NPs and Fe_3O_4 NPs are well combined in synthesizing Fe_3O_4@Ag NCs. As calculated from TEM images, the average particle size of Ag NPs is 23 nm while that of Fe_3O_4 NPs and Fe_3O_4@Ag NC are 11nm. Adsorption study of methylene blue (MB) using Fe_3O_4 NPs was done and maximum absorbance of 91.72% was obtained at 100 min starting with $4x10^{-4}$M MB dye solution and using 40 mg of adsorbent. Photodegradation study of MB dye solution was done using AgNPs and Fe_3O_4@AgNC as catalyst. The result indicated that Fe_3O_4@Ag NC has higher degradation efficiency and reusability advantage than AgNPs. Kinetic study showed that the catalyst best fit to Pseudo second order than pseudo first order kinetic model. Fe_3O_4 NPs, Ag NPs and Fe_3O_4@Ag NC demonstrated high-antibacterial activity against Staphylococcus aureus as evaluated by means of inhibition zone than Escherichia coli.

Keywords: Essential Oil, *Solanum Incanum*, silver nanoparticles, magnetite nanoparticles, nanocomposite, methylene blue. Antibacterial activity, Photodegradation.

Chapter One

1 Introduction

1.1 Background of Study

Nanotechnology is a field of science that deals with the synthesis and development of various nanomaterials [1] that range from 1nm -100 nm by size [1, 2]. In the scientific world, nanoparticles get a great attention due to their large surface area to volume ratio, high reactivity [3], high thermal, electrical conductivity, their demonstrated catalytic activity and their biocompatibility [4]. Among these iron oxide Nanoparticle gets significant technological attention due to its magnetic property and different potential application. Combining of these magnetic nanomaterial with an optically active material such as silver, makes them quite efficient to be used as multimodal agents in application [5] such as in electronics, photonics, catalysis and biomedicine [6]. There are three basic methods for the synthesis of nanoparticles named physical, chemical and biological methods [7]. Biosynthesis is an inexpensive, faster eco-friendly and nontoxic method for the preparation of the nanoparticles. There are many biological resources for the synthesis of nanoparticles like plant extract, fungus, bacteria, and algae, etc [8]. There has been a rapid increase in using natural products like plant materials extract for synthesis of nanomaterials [9, 10].

In modern pharmaceutical science, the extent of the degree of interest has been shifted more towards the herbal products as compared to synthetic products due to better affordability, acceptability, and compatibility with human physiology and minimal side effects [11]. *Solanum incanum (L)* is important traditional medicinal plant that belongs to the *Solanaceae* family [12]. The plant is a common shrub in Ethiopia, found in left-over agricultural lands, roadsides, and village yards. The plant has different local names in Ethiopia such as Embuay (by Amharic) and Hiddi (by afaan Oromo). Different parts of the plant are traditionally employed as medicine, the fruits and fresh leaves are applied for tropical ulcers and to stop bleeding; the root is used for syphilis, leprosy, and gonorrhea [13]. *Solanum incanum (L)* comprises essential oil which is a volatile compound that plays very important roles in plant defense and signaling processes [14].

Present work focuses on the extraction of Essential Oils from *Solanum Incanum (L)* root by using Steam distillation, and analysis by GC-MS. Essential oil mediated synthesis of Fe_3O_4 NPs, Ag NPs and Fe_3O_4@Ag NC for antibacterial (inhibiting pathogenic Escherichia coli and Staphylococcus

aureus) application. In addition, Elimination of environmental pollutants, in particular, toxic dyes, has remained as a major challenge over the years [15]. Hence, degradation of methylene blue (MB) using hydrogen peroxide (H_2O_2) have been chosen as probe reactions to demonstrate the catalytic action of the synthesized Fe_3O_4 NPs, Ag NPs and Fe_3O_4@Ag NC.

1.2 Statement of the Problem

In the past silver nanoparticles (Ag NPs) have been extensively used in various applications including catalysis, metal electrodes, biotechnology and bioengineering. Currently, Ag NPs or their composites have been employed as effective antibacterial agents in a diverse range of consumer products. Unfortunately, Ag NPs synthesized using conventional methods aggregate easily, which greatly decreases their antibacterial activity. To solve this problem, AgNPs have been loaded onto suitable matrix. Fe_3O_4 NPs have found a lot of applications in various fields. Combining Fe_3O_4 NPs and Ag NPs can not only prevent the coalescence of Ag NPs, but also achieve recycling of nanosized silver to avoid contamination of surroundings [16]. Such nanocomposite could lead to interesting advances to solve the lack of biocompatibility of silver, eliminating its contact with tissues (iron oxide can be considered biocompatible, at least up to the mg/ml range) [17]. Methylene blue largely has been used in human and veterinary medicine for several therapeutic and diagnostic procedures. It cannot be degraded through the conventional water treatment process due to its complex aromatic structures, hydrophilic nature, and high stability against light, temperature, water, chemicals, etc. and it may cause substantial environment pollution [18] and Pathogenic food-borne bacteria such has S. aureus and E. coli have been associated with severe morbidity and mortality in humans and animals [19]. Different researchers have done on the synthesis of Fe_3O_4 NPs, Ag NPs and Fe_3O_4@Ag nanocomposite for antibacterial applications and catalytic degradation. However green method using *Solanum incanum* plant essential oil as reducing agent *against* human pathogenic bacteria has not been reported yet. Hence, this study intended to use EOs from *Solanum incanum (L)* root to synthesis Fe_3O_4 NPs, AgNPs and Fe_3O_4@Ag nanocomposite and then apply the synthesized nanomaterials in removal of dye pollutant and disinfection of bacteria.

1.3 Objectives

1.3.1 General Objective

The general objective of this work is extraction of essential oils from *Solanum Incanum (L) root* using steam distillation and synthesis of EO mediated Ag NPs, Fe_3O_4 NPs and Fe_3O_4@Ag NC for degradation of methylene blue and antibacterial application.

1.3.2 Specific Objectives

The specific objectives are:

- To extract the essential oils from the root of *Solanum incanum (L)* using steam distillation.
- To analyze the qualitative composition of the extracted essential oil.
- To Synthesize Fe_3O_4 NPs, Ag NPs and Fe_3O_4@Ag NC through green method using *Solanum incanum (L)* EO as a reducing agent.
- To Investigate the synthesized Fe_3O_4 NPs, Ag NPs and Fe_3O_4@Ag NC using FTIR, XRD, SEM-EDX, TEM and UV-visible spectroscopy.
- To investigate Adsorption methylene blue removal efficiency of Fe_3O_4 NPs,
- To investigate degradation of methylene blue removal efficiency of Ag NPs and Fe_3O_4@Ag NC
- To investigate the antibacterial activity of Fe_3O_4 NPs, Ag NPs and Fe_3O_4@Ag NC

1.4 Scope of the Study

The scope of the study is limited to green synthesis Fe_3O_4 NPs, Ag NPs and Fe_3O_4@Ag NC using *Solanum incanum (L)* root extracted EO and characterization of the synthesized nanomaterials using UV-VIS XRD, FTIR, and SEM-EDX technique and investigation of methylene blue removal efficiency and antibacterial activities against two bacteria, S. aureus and E. coli.

1.5 Limitations of the Study

This study able to produce only laboratory scale test samples and unable to do more characterization due to unavailability of VSM and XPS instrument in the country and due to condition related with COVID-19, TGA could not be characterized.

1.6 Significance of the Study

This study could provide important information about the green synthesis strategy of Fe_3O_4NPs, Ag NPs and Fe_3O_4@Ag NC using essential oil as reducing agent and their antibacterial and catalytic activity.

Chapter Two

2 Literature Review

2.1 Essential Oil and Its Property

Essential oils are volatile, complex, natural compounds characterized by a strong odor and formed by aromatic plants as secondary metabolites [9, 20, 21]. Essential oils are commonly used as flavoring agents in food products, drinks, perfumeries, pharmaceuticals and cosmetics [21]. EO, named as aromatic oils, fragrant oils, steam volatile oils, ethereal oils [22]. Essential oils are separated from the aqueous phase by a physical method, that does not lead to significant change in its chemical composition [23].

In aromatic plants, the composition of EO usually varies considerably because of both intrinsic (sexual, seasonal, ontogenetic, and genetic variations) and extrinsic (ecological and environmental aspects). EO quality strongly depends on all these factors that may interfere and also limit plant yield. Genetic variations may result in the expression of different metabolic pathways and, consequently, made quantitative and qualitative variations in essential oil composition[14]. EO can be classified into four main groups (1) Terpenes, (2) Straight chain compounds not containing any side chain (3) Phenylpropanoids (benzene derivatives) (4) Miscellaneous group having varied structures not included in first three groups (sulfur or nitrogen containing compounds) [24].

2.2 Essential Oil Extraction Using Steam Distillation

Common techniques used for the extraction of essential oils are hydro-distillation, Hydro diffusion, Effleurage, Cold pressing, Steam distillation, solvent extraction, Microwave-Assisted Process (MAP) and Carbon dioxide extraction [25]. On a commercial scale, steam distillation is a preferred method for the extraction of EOs [9].

Steam distillation is a type of distillation (a separation or extraction process) for a temperature sensitive plant such as natural aromatic compounds [22].. Which is a simplest method of extracting EO [26, 27]. It is a method where steam flows through the material as shown in fig 1 [28]. This steam functions as agents that break up the pores of the raw material and release the essential oil from it. The system yields a mixture of a vapor and desired essential oil. This vapor is then condensed further [22]..

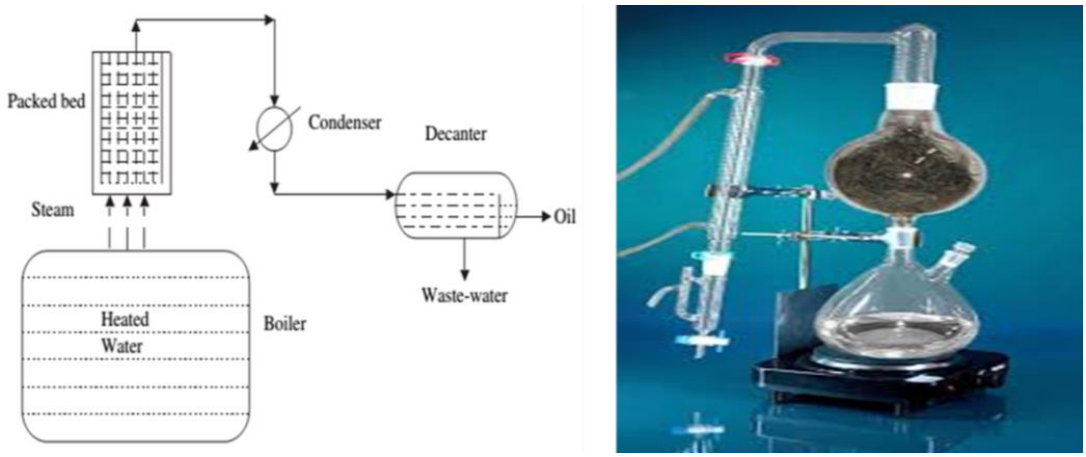

Figure 1: Schematic diagram for steam distillation extraction process.

2.3 Analysis of Essential Oils

GC-MS is a combination of two different analytical techniques, Gas Chromatography (GC) and Mass Spectrometry (MS). GC-MS used to analyze complex organic and biochemical mixtures. The GC-MS instrument consists of two main components. The gas chromatography portion separates different compounds in the sample into pulses of pure chemicals based on their volatility by flowing an inert gas (mobile phase), which carries the sample, through a stationary phase fixed in the column. Spectra of compounds are collected as they exit a chromatographic column by the mass spectrometer, which identifies and quantifies the chemicals according their mass-to-charge ratio (m/z). These spectra can then be stored on the computer and analyzed [29]. Mass spectrometry is the preferred detection system for the identification of EO components. The combination of GC and MS results in a very powerful tool for EO chemical characterization [30].

2.4 Nanoparticles and Their Property

Nanoparticles are of great scientific interest as they are a bridge between bulk substances and their molecular or atomic structure. A bulk substance has constant physical and chemical properties irrespective of its size; nevertheless, at the nanoscale these properties depend more or less on particle size [31].

2.4.1. Surface Area and Size

It has been found that properties vary with particle size. Particle size and surface area play a major role in interaction of materials with biological system. Seemingly, decreasing the size of the materials leads to an exponential increase in surface area to volume ratio, thereby making the nanomaterial surface more reactive [31]

2.4.2 Optical Properties

One of the most fascinating and useful aspects of nanomaterials is their optical properties. Applications based on optical properties of nanomaterials include optical detector, laser, sensor, imaging, phosphor, display, solar cell, photocatalysis, photo electrochemistry and biomedicine [32]. Noble metal nanoparticles (NPs), especially made of Ag and Au, have been attracting a great deal of attention due to their size and shape dependent optical properties which arise from their surface plasmon resonances [33]. As the size decreases, the specific surface area increases and a quantum effect appears that leads to profound changes in the properties of materials. Since optical properties depend on the internal electronic structures of nanomaterials, thus investigation of optical properties of nanomaterials can give us deep understanding of their structure [34].

2.4.3. Magnetic Property

Magnetic effects are caused by movements of particles that have both mass and electric charges. These particles are electrons, holes, protons, and positive and negative ions. Materials are classified by their response to an externally applied magnetic field. Industrial applications of magnetic nanoparticles cover a broad spectrum of magnetic recording media and biomedical applications, for example, magnetic resonance contrast media and therapeutic agents in cancer treatment Akbarzadeh, Samiei [35]. Iron oxide are widely used in magnetic and biomedical application including contrast agents, drug delivery and hyperthermia [36].

2.5 Approaches for the Synthesis of Nanoparticles

There are two general approaches for synthesis of nanomaterials; top-down and bottom-up approach [37, 38]. These approaches further divide into various subclasses based on the operation, reaction condition and adopted protocols [38]. Fig. 2 shows bottom up and top down approaches subclass:

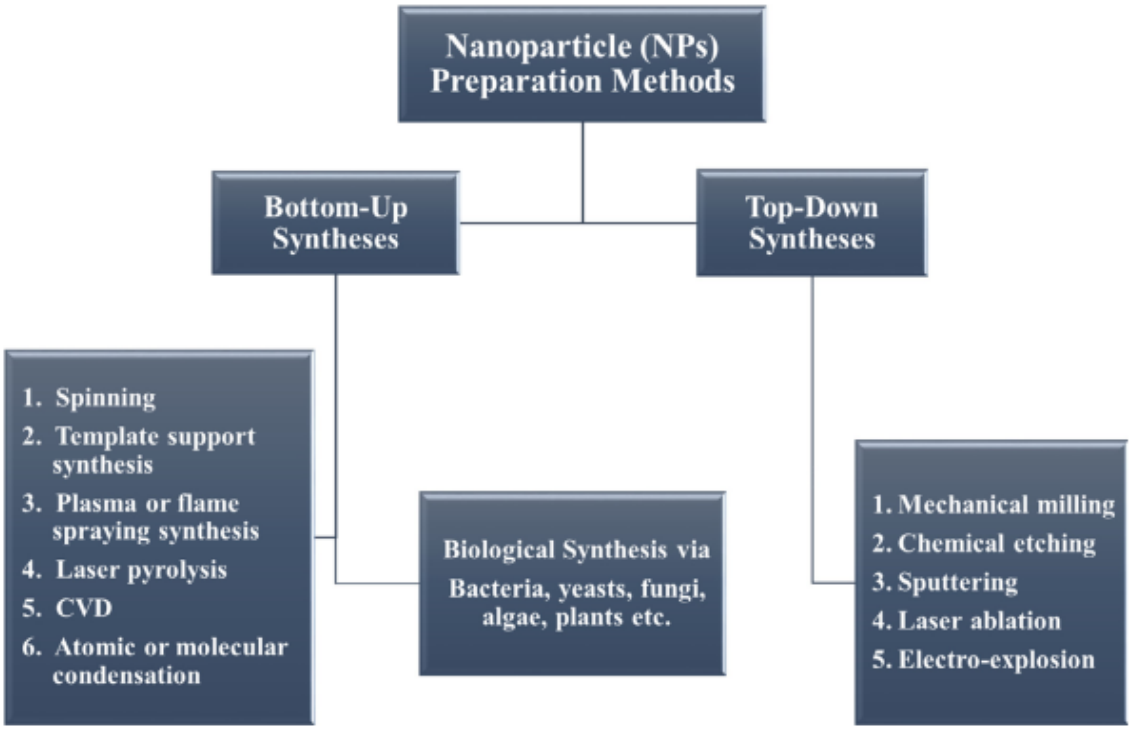

Figure 2: Approaches for the synthesis of nanoparticles.

From fig. 2 top down approach is destructive approach starting from larger molecule, which decomposed into smaller units and then these units are converted into suitable NPs. Examples of this method are grinding/milling, physical vapor deposition (PVD) and other decomposition techniques [38].

Bottom up approach is employed in reverse as NPs are formed from relatively simpler substances, therefore this approach is also called building up approach. Examples of this case are sedimentation and reduction techniques. It includes sol gel, green synthesis, spinning, and biochemical synthesis [38]. In another way, there are three basic methods for the synthesis of nanoparticles named physical, chemical and biological methods. Further classifications of those methods are given in Table 1.

Table 1: Methods for the synthesis of nanoparticles.

Physical Method	Biological (Green) Method	Chemical Method
Arc discharge method	By Plant extract	Co-Precipitation Method
Electron beam lithography	By Microorganisms	Sono-chemical Method
Ion implantation	By Algae	Electrolysis
Inert gas condensation	By Biomolecules or Enzymes	Microemulsion Method
Mechanical grinding	By Agricultural and Industrial Waste	Chemical reduction Method
Spray pyrolysis		Phytochemical Method
Vapor phase Synthesis		Sol-gel Method
		Pyrolysis
		Solvothermal/Hydrothermal Method

Physical and chemical methods listed in Table 1 are widely used for the synthesis of nanoparticles, unfortunately, these methods have some drawbacks such as their use of high energy or hazardous chemicals, great expense and production of large amounts of toxic byproducts that create environmental contamination. To overcome these limitations of physical and chemical methods, ecofriendly, facile, low cost and nontoxic methodologies are essential for metal nanoparticle synthesis by avoiding the use of toxic and expensive chemicals and solvents. Recently, biological synthesis of metal nanoparticles has been highlighted, which is safe, ecofriendly, facile, nontoxic and economical [7].

2.6 Green Synthesis of Nanoparticle

Green (Biosynthesis) synthesis of nanomaterials means the synthesizing of nanomaterials or nanoparticles without using hazardous chemicals that produce toxic by-products[39]. Biosynthesis is an inexpensive, faster eco-friendly and nontoxic method for the preparation of the nanoparticles. There are many biological resources for the synthesis of nanoparticles like plant extract, fungus,

bacteria, and algae, etc. Plant extracts are preferable for the synthesis of the nanoparticles than other microorganisms because they are abundantly avaliable and have chemical components which can act as good reducing agents [8].

Biosynthesis of nanoparticles employs the bottom-up approach where the metal atoms assemble to form clusters and then eventually the nanoparticles. The biological compounds present in green materials may act as both reducing and capping agents that can stabilize the nanoparticles during the synthesis process. This can control the size and shape of the nanoparticles which can be used in various applications [39].

2.6.1 Green Synthesis of Fe_3O_4 Nanoparticles

Magnetic (iron-oxide) nanoparticles have been synthesized by various methods, including thermal decomposition, vacuum sputtering, co-precipitation, hydrothermal, and chemical reduction methods [40]. Coprecipitation methods are simple and allow the preparation of magnetic NPs with rigorous control of size and shape. Homogeneous precipitation reactions are used to synthesize uniform sizes that involve the separation of the nucleation and growth of the nuclei [41]. Co-precipitation method offers advantages such as simple and rapid preparation, easy control of particle size and composition, various possibilities to modify the particle surface state and overall homogeneity, low temperature, energy efficient, and does not involve use of organic solvent [42].

Green production of Fe_3O_4 NPs is the process in which plant extracts, microorganisms (bacteria, fungi, algae, and yeast), and enzymes play a significant role in Fe_3O_4NPs synthesis from naturally biodegradable matter. Among these, synthesis by plant extracts is advantageous because it reduces the risk of further contamination by decreasing the reaction time and maintaining the cell structure [43].So due those advantage this study intended to use Essential oil from *Solanum incanum* plant and synthesis of iron oxide nanoparticle.

2.6.2 Green Synthesis of Silver Nanoparticles

Among the metallic nanoparticles, silver nanoparticles (Ag NPs) in particular are known for their versatile biological applications in the fields of medicine and biotechnology. Recently, biological methods for synthesis of Ag NPs have been developed because they are eco-friendly and cost-

effective. With advances in the green chemistry approach, biological synthesis of Ag NPs has been focused on as a substitute to physical and chemical processes, and offers budding opportunities for synthesis of Ag NPs. Several biological materials such as microorganisms, plant extracts, and milk have been used for the synthesis of Ag NPs. Synthesis of Ag NPs using plant extracts is potentially advantageous over microorganisms because of its simple scale up [44].

Recently different researcher synthesize silver nanoparticle from different plant essential oil for various applacation some of them are, R.R.Thanighaiarassu et al synthesize AgNPs using essential oil compound citral for antifungal activity [45], Ramya et al. 2018 synthesize Ag NPs using essential oil compound Geraniol for antifungal Activity [46], R.R. Thanighai arassu et al.2018 synthesize Ag NPs using essential oil from rosemarinus officinalis plant for antifungal Activity [47], Vidya Vilas et al. synthesize Ag NPs from C. aromaticus essential oil for environmental, anti-microbial and antioxidant applications [48].

2.6.3 Green Synthesis of Fe_3O_4@Ag Nanocomposite

Composites are the materials that consist of two or more chemically and physically different phases separated by a distinct interface. Nanocomposites are a relatively new class of materials with ultrafine phase dimensions, typically of the order of a few nanometers. Nanocomposites are the composites which are size dependent with at least one of the phases shows dimensions in the nanometer range and are different from those of the atomic and bulk counterparts. The size plays a vital role in the nanocomposites with unique properties typically not shared by their micro composite and, therefore, offer new technology and business opportunities. According to the type of matrix materials that are used for the preparation of nanocomposites, the nanocomposites are classified into following three classes: Polymer Matrix Nanocomposites, ceramic Matrix Nanocomposites and Metal Matrix Nanocomposites [49].

There are several chemical and physical methods for the preparation of metal/Fe_3O_4 magnetic nanoparticles. However, these methods have disadvantages such as utilization of organic solvents, harsh reaction conditions (high temperature and pressure) and use of expensive and toxic reducing agents, use of expensive capping agents and organic surfactants, which make them environmentally and economically malignant. Therefore, the development of a simple and environmentally friend method for the preparation of magnetic nano catalysts has been a major challenge [50].

Considering preparation based on precipitation, one and two-stage processes can be used to synthesis Fe_3O_4@Ag nanocomposite. In the one-stage synthesis silver nitrate solution is added to a solution containing iron (III) and iron (II) salt in the help reducing and oxidizing agent. A suspension formed is then reacted at high temperature in an autoclave [51]. In the two-stage method, Fe_3O_4 nanoparticle is initially prepared and coated with silver. Plant extract may be used as a mild reducer to coat magnetic nanoparticles of iron (II)(III) oxide with a silver layer. Finally the magnetic nanoparticles of Fe_3O_4@Ag nanostructure are separated with a magnet [52]. Due to non toxicity, fast, low temprature and ecofriendly of two-stage process this study inteded to use two stage method.

2.7 Essential Oil For Nanoparticle Synthesis

Nanotechnology is expected to open some new ways to fight and prevent diseases using atomic scale tailoring of materials. There are a lot of reports on the antimicrobial and antibiofilm properties of different types of nanoparticles, especially heavy metal containing ones (silver, copper, gold and ZnO), as well as the core/shell nano systems (e.g., $CoFe_2O_4$/oleic acid, Fe_3O_4/oleic acid and Fe_3O_4/PEG600) [53]. Biomolecules including polyphenols, saponins, proteins and terpenoids present in plants play active role in reduction of inorganic metal ions and their consequent stabilization [54].

The essential oils are an interesting alternative for the antimicrobial therapy, acting by multiple mechanisms, including cell wall damages, inhibiting the cell wall or protein synthesis, or interfering with intermediary metabolisms or DNA/RNA synthesis/function [55]. However, like other EOs, are volatile compound which easily evaporates and/or decomposes during food processing, drug formulation, and preparation of antimicrobial film, etc., owing to direct exposure to heat, pressure, light or oxygen. In order to overcome the susceptibility and improve the stability of bioactive compounds during processing and storage, the emerging technology of nano-encapsulation has been recently applied in food and nutraceutical industries. Nanoencapsulation of bioactive compounds represents a viable and efficient approach to increase the physical stability of the active substances, protect them from the interactions with the food ingredients and enhance their bioactivity, because of the subcellular size [56]. Due to instability of essential oil preparing with stable and non-toxic material like nanoparticle is very important to increase stability.

2.8 Antibacterial Strains

Staphylococcus aureus and Escherichia coli account for the majority of clinical mastitis cases in cattle, whereas, S. aureus is the most prevalent pathogen associated with human mastitis[57, 58]. Striking differences exist between the courses of bovine intramammary infection caused by S. aureus and E. coli. Intramammary infection by E. coli is acute in nature and generally clears within a few days. In contrast, infection by S. aureus is often less severe but results in a chronic infection that can persist for the life of the animal [57]. So, developing resistant with biocompatible application material is very important to save life from those bacteria.

2.9 Application of F_3O_4-Ag Nanocomposite

2.9.1 Antibacterial Activity of F_3O_4@Ag Nanocomposite

Currently, AgNPs and their composites have been employed as effective antibacterial agents in a diverse range of consumer products [16]. The antibacterial mechanism of AgNPs is associated with the release of silver ions [59]. Formation of Fe_3O_4@Ag composite type improved allows to combine the magnetic properties of the iron oxide with the bactericidal and bacteriostatic properties of the silver [60]. Different researchers synthesize Fe_3O_4@Ag composite for antibacterial activity some of theme are [61], [62]

2.9.2 Catalytic Activity

It is well known that metal nanoparticles have potential to catalyze some chemical reactions that are not achievable. The size, shape, and composition of nanoparticles play an important role in the catalytic reactions [40]**.** Homogeneous catalysts suffer from disadvantages such as high operational costs, short life time, labor-intensive and the difficulty of separating from the reaction mixture. These problems affect reaction yields and recycle activity of the catalyst which lead to environmental problems and restrict their application in synthesis due to environmental concerns and industrial processes. According to the points of green chemistry, the use of inexpensive and non-corrosive heterogeneous catalysts presents a promising option, so, due to safety considerations [50].

Among heterogeneous catalysts, magnetic nano catalysts are attractive candidates as effective catalysts for the highly active and recyclable catalytic systems. The beneficial applications of these catalysts are mainly due to their unique magnetic, electronic, and catalytic properties, excellent

chemical stability, low cost, huge industrial applications and large surface area. In addition, these catalysts can be separated from the reaction medium and recovered for using in next reaction cycles easily through an external magnetic field without using any centrifugation or filtration [50]. Many researchers work on catalytic removal of dye some of them are [63], [64].

2.8.3.1 Methylene Blue

Organic dyes are generally used in industries like plastic, paper, pharmaceutical, cosmetic, food, and textile. They pose potential hazard to our environment and water bodies. Most commonly used organic dyes in industries includes methylene blue, methyl red, Congo red, methyl orange, eosin Y, bromophenol blue, acridine orange, phenol red, etc. [65]. Organic dyes have received particular attention as prominent environmental contaminants owing to their non-biodegradability and carcinogenic effects on humans [66]. Methylene blue is used dye paper and office supplies but also to tone up silk colors. It has largely been used in human and veterinary medicine for several therapeutic and diagnostic procedures. It cannot be degraded through the conventional water treatment process due to its complex aromatic structures, hydrophilic nature, and high stability against light, temperature, water, chemicals, etc., and it may cause substantial environment pollution [67].

Chapter Three

3. Material and Methods

3.1 Material

3.1.1 Chemicals

In the study anhydrous sodium sulfate was used for drying essential oil, Silver nitrate ($AgNO_3$) (SCHULU CHEMIE SA LA. JOTA BARCELONA L 98%) was used as precursor of silver nanoparticles, Iron (II) Sulphate Heptahydrate ($FeSO_4.7H_2O$, 87%) (SAMIR TECH-CHEM PVT LTD) and Iron (III) nitrate nonahydrate ($Fe(NO_3)_3$).9H2O, 98% (UN-CHEM CHEMICAL REAGENT) were used as precursor of iron oxide nanoparticles, NaOH (sodium hydroxide (CENTRAL DRUG HOUSE(P) LTD) was used to adjust pH and for completion of reaction, Methylene blue (SAMIR TECH-CHEM, PVT, LTD) was used as representative dye pollutant, H_2O_2 (FINE CHEMICAL GENERAL TRADING, 30%) was used in degradation of methylene blue.

3.2 Methods

3.2.1 Collection and Pretreatment of Plant Sample

A total of 12 kg of the *Solanum incanum* (L) root was collected from Adama Science and Technology University. The impurities (dust and soil on the plant material) were removed by repeated washing with tap water and finally with distilled water. The *Solanum incanum* (L) root was used freshly for essential oil extraction.

3.2.2 Extraction of *Solanum Incanum* (L) Essential Oil

The extraction of Essential oil (EO) was conducted using the steam distillation method. For experimental work, 200 gm of chopped and grinded *Solanum incanum* (L) root was used. Before the operation start the steam, distillation setup was cleaned. *Solanum incanum* (L) root was loaded on to column and distilled water was added to the round bottom flask. The boiler was used to generate steam and let to enter into the column to extract the required amount of essential oil. Volatile components separated, then condensed with cold water and collected in separate flask. The experiment was carried at 75 ^oC for 3 hrs. Finally, the collected condensate mixture was separated by separatory funnel using hexane as organic solvent, dried using rotavapor and then

using sodium sulphate, quantitatively analyzed using GC-MS and the essential oil used for synthesis of nanomaterials [68].

3.2.3 Gas Chromatography/Mass Spectroscopy (GC-MS) Analysis

The EO was analyzed by GC-MS using column (30 m× 0.25 mm; film thickness 0.25 µm). The carrier gas was helium with a flow rate of 1 mL/min (split ratio of 1:10) and the injector at 260°C. Injected sample volumes were 1µl. Temperature was programmed from 60 °C to 280 °C at 3 °C/min ramping. The ionization energy was 70 eV, and the mass range m/z was 20–550. The components were identified by their mass spectra and retention indices. The mass spectra were compared with library to identify compound in essential oil.

3.2.5 Green Synthesis of Ag Nanoparticle Using Essential Oil.

Ag NPs was synthesized using essential oils of Solanum incanum (L) root as reducing and capping agents. 100 mL of 1:1 volume ratios of the essential oils and 1mM $AgNO_3$ solution was added in 250 mL round bottomed flask, under stirring for 15 min. Then, 10 mL of 1.0 M NaOH solution was added to the reaction mixture and the reaction mixture was refluxed for 1 hr under constant magnetic stirring. When the color of the reaction medium turned to amber color, formation of Ag NPs was confirmed. Ag NPs formed separated with centrifugation at around 3500 RPM and then decantation and washed with deionized water three times to remove any unreacted essential oils. The prepared Ag NPs was dried in drying oven at 105^{o}C for 24 hrs [69].

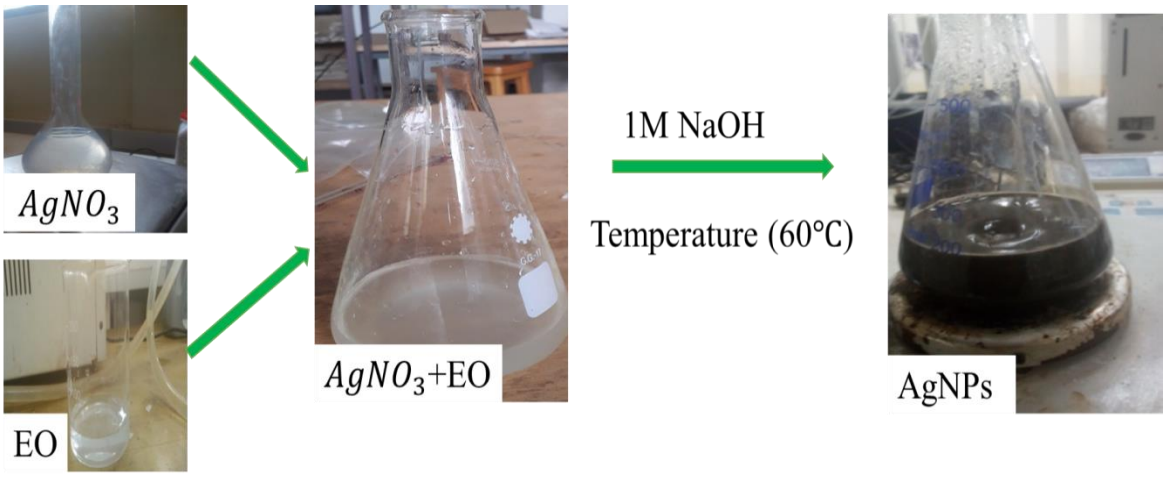

Figure 3: Diagram showing synthesis process of Ag NPs

3.2.4 Green Synthesis of Fe_3O_4 Nanoparticle Using Essential Oil

For the synthesis of Fe_3O_4 NPs using essential oil of *Solanum incanum*(L) root, firstly, 2:1 mole ratio of Fe^{3+} and Fe^{2+} respectively, was prepared by mixing aqueous solution of Iron (II) sulphate and Iron (III) nitrate. The prepared Fe^{3+} to Fe^{2+} aqueous solution was mixed with 50mL of EO with stirring, closing by condenser to keep EO compounds from evaporation, and heating at 60°C temperature until yellow color appears. Then freshly prepared 1.0 M of NaOH was added drop-wise to the obtained color-suspension under continuous stirring until black color appear. The pH of the solution was adjusted to pH 11 and the solution was stirred for 1 hr to homogenize the solution and also for the completion of reaction. After separation by using a permanent magnet, synthesized Fe_3O_4 NPs was washed for several times by using deionized water. The synthesized nanoparticles were dried in an oven at around 105°C for 24 h. The dried sample was stored in an air tight container for further use and characterization [70].

3.2.6 Green Synthesis of Fe_3O_4@Ag Nanocomposites

Two stage methods were used to prepare Fe_3O_4@Ag Nanocomposite. 2 grams of the previously synthesized Fe_3O_4 nanoparticles was taken in 50 mL of aqueous essential oils solution and stirred for 20 minutes. Then 50 mL of 1mM silver nitrate solution was added and stirred for 15 minutes. Finally, 10 mL of 1.0 M NaOH solution was added to the reaction mixture and the reaction mixture was refluxed for 1 h under constant magnetic stirring. As formed Fe_3O_4@Ag Nanocomposite was separated with help of external magnet and washed with deionized water three times to remove any unreacted impurities [52].

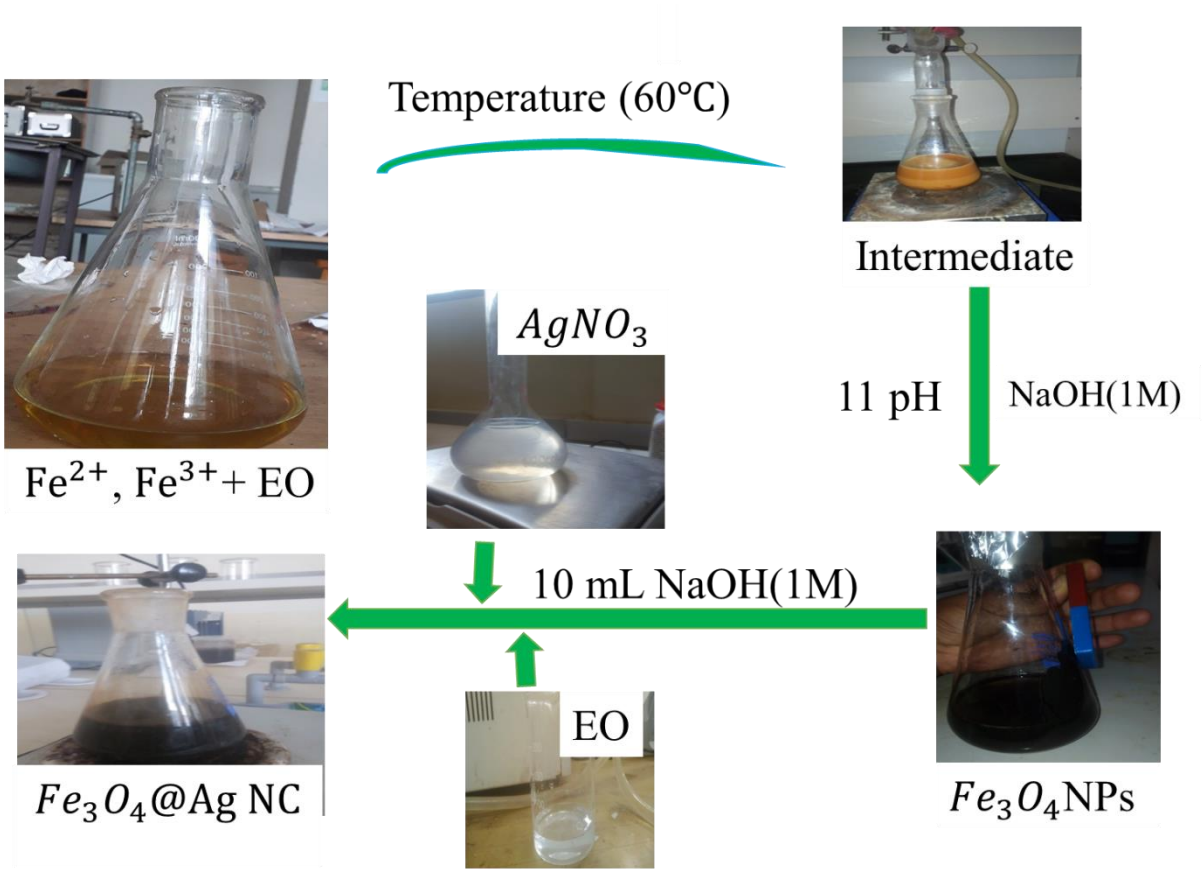

Figure 4: Diagram showing synthesis process of Fe_3O_4 NPs and Fe_3O_4@Ag NC

3.2.7 Characterization Techniques

The prepared samples were primarily characterized by UV-Vis spectrophotometer (Labomed Model UVD-2950). 3 mL of the solution was taken in a cuvette and scanned using double beam UV-Vis-spectrophotometry from 200 nm to 800 nm wavelength. FTIR spectrometer (JASCO FTIR 400) was used to determine the functional groups in the synthesized nanomaterials. Powder X-ray diffraction (XRD) pattern of synthesized nanomaterials were determined by X-ray diffraction (XRD) analysis using a Rigaku D/MAX 2500 with Cu Kα radiation. Transmission electron microscopy (TEM, JEOL model 3010 microscope) operated at an accelerating voltage of 200 keV with wavelength of 0.0251A˚ was used to determine morphology and particle size of synthesized nanomaterials. The morphology and elemental composition of the samples were characterized using scanning electron microscopy (SEM, Zeiss Ultra-60) equipped with X-ray energy dispersive spectroscopy (EDS).

3.2.8 Catalytic Removal of Methylene Blue

The catalytic activity of synthesized Fe_3O_4 NPs, Ag NPs and Fe_3O_4@Ag NC were tested using methylene blue (MB) as representative organic dye pollutant. In this typical process, 3 drops of 30% H_2O_2 solution were mixed with 100 mL of MB dye solution ($4x10^{-4}$M) in a glass beaker and stirred vigorously for 2 min on a magnetic stirrer. To the above mixture, 40 mg of the Fe_3O_4 NPs, were added and while stirring 3mL of solution taken at 20-minute time interval from starting to 120 minutes for recording the remaining MB in the solution. The extent of adsorption and degradation was evaluated by measuring the absorbance at the λ_{max} = 665 nm of MB. The amount of MB adsorbed during the adsorption process and the percentage degradation of MB using Fe_3O_4 NPs were calculated by equation. 1 and 2, respectively. Kinetic study and efficiency of catalyst was done according to [64] and [71].

The photodegradation experiment was performed by adding 40 mg of catalyst and 3 drops of 30% H_2O_2 solution to 100 mL of the dye solution (4×10^{-4} M). The suspension was magnetically stirred in the dark for 30 minutes in order to attain adsorption-desorption equilibrium before the irradiation by UV light. The main advantage of using the UV light was to produce electron and hole pair (e^-/h^+) with high energy state that migrate to the nanoparticle surface and initiate a wide range of chemical reactions [72].

$$Q = \frac{(C_t - C_o)}{m} xV \quad \text{..... (eq. 1)}$$

$$\% \text{ Degradation} = \frac{(A_0 - A_t)}{A_0} x100 \quad \text{.....(eq. 2)}$$

Where Q (mg/g) is the amount of MB adsorbed on the surface of Fe_3O_4 NPs, C_0(mg/L) is the initial concentration of dye before adsorption, C_t(mg/L) the concentration MB at a time 't', V(mL) is a volume of MB, m(g) is mass of nanomaterial catalyst, A_o and A_t are the absorbance of MB after t time adsorption and degradation, respectively. The same calculation for Ag NPs and Fe_3O_4@Ag NC also.

3.2.9 Assessment of Antibacterial Activity

The antibacterial activity was done on *Escherichia coli* and *Staphylococcus aureus* by using the standard disc diffusion method. On available broth, medium was used to subculture bacteria and was incubating at 37 ℃ for 24 hrs. Fresh overnight cultures was taken and spread on the agar plates

to cultivate bacteria. Sterile paper discs of 6 mm diameter saturated with nanomaterials, essential oil, and double-distilled water (as negative control) and the antibacterial activity was measured based on the inhibition zone around the disc impregnated with nanomaterials and essential oils.

Chapter Four

4 Results and Discussion

4.1 GC-MS Analysis of Essential Oil

Essential oil chemical components were identified by a GC–MS spectrometer with a fused-silica column (DB5, 30 m×0.25 mm) and composition of their mass spectra and fragmentation patterns were identified using NIST library. (Fig. 3) shows GC-MS total ion chromatogram of essential oil of *Solanum incanum* root. The identified components from essential oil of *Solanum incanum* root are given in table 2. These different components of EO are responsible for reduction and capping of synthesized nanomaterials.

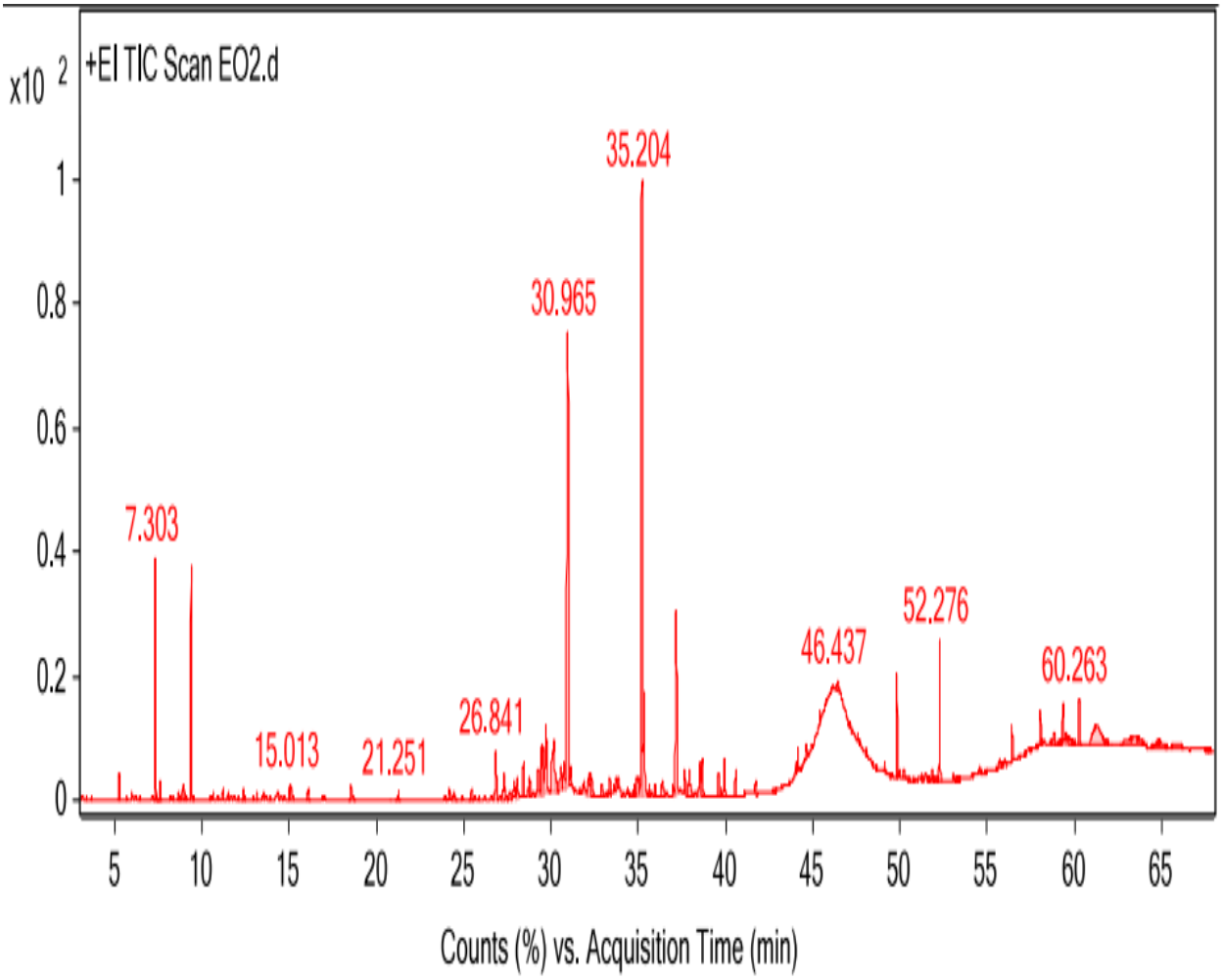

Figure 5 : GC-MS spectrum of *Solanum incanum (L)* root Essential Oil

Table 2: Major component of essential oil from *Solanum incanum(L) root*

Number	Identified compound	Chemical formula	RT	Peak area (%)
1	Benzyl alcohol	C_7H_8O	7.303	3.44
2	Benzene ethanol	$C_8H_{10}O$	9.371	3.48
3	6-isopropenyl-4-8a-dimethyl-1,2,3,5,6,7,8a-octahydro-naphthalen-2-ol	$C_{12}H_{17}NO_2$	29.694	3.21
4	2-(2R,4aR,8as) -4a-methyl-8-methylenedecahydronaphthalen-2-yl) prop-2-en-1-ol	$C_{10}H_8N_2O$	30.168	3.06
5	7R,8R,8-hydroxy (-4-isopropydene-7-methyl [bicyclo [5,3,1] uner-1-ene	$C_{15}H_{24}O$	30.965	17.69
6	7-isopropenyl-4a-dimethyl-4a,5,6,7,8-hexahydro-3H-naphthalen-2-one	$C_{15}H_{22}O$	35.204	16.12
7	2-(3H)-Naphthalenone,4,4a,5,6,7,8-hexahydro-4,4a-dimethyl-6-(1-methylethenyl)- [4R-(4-alpha, 4a, alpha,6, beta	$C_{15}H_{22}O$	35.337	2.88
8	Murdan-3,9(11)-diene-10-peroxy	$C_{15}H_{24}O_2$	37.168	6.01
9	1,2-benzenedicarboxylic acid, 1,2-bis(2-ethylhexyl) ester	$C_{24}H_{38}O_4$	52.276	2.47
10	2-propanoic acid decylester	$C_{21}H_{40}O_4$	61.257	2.98
11	Dasycarpidan-1-methanol acetate(ester)	$C_{15}H_{24}N_2O_2$	63.446	2.41

4.2 Fe_3O_4 NPs, Ag NPs and Fe_3O_4 @ Ag NC Synthesis

In this study Fe_3O_4 NPs, Ag NPs and Fe_3O_4@Ag NC were prepared by green approach using essential oil of *Solanum incanum (L)* root as reducing and capping agent. All Fe_3O_4 NPs, Ag NPs and Ag@Fe_3O_4 NC were prepared under alkaline conditions at room temperature. During Fe_3O_4NPs preparation the color of the reaction mixture of Fe^{+3} and Fe^{+2} salts and *Solanum incanum(L)* EO changed from yellow to brown black (Fig. 4) after addition of NaOH and stirring the solution for 1hr, which indicates the formation of Fe_3O_4 NPs. The synthesized Fe_3O_4 NPs is able to be attracted by an external permanent magnet quickly which proved that the nanoparticles possessed magnetic properties. Once the magnet removed, the nanoparticles were dispersed readily. The plausible chemical reaction for the formation of Fe_3O_4 NPs is as follows [73]:

$$2Fe^{3+} + Fe^{2+} + 8OH^- \rightarrow 2Fe(OH)_2Fe(OH)_2(s) \rightarrow Fe_3O_4(s) + 4H_2O \quad \text{..... (eq. 3)}$$

Ag NPs was synthesized using $AgNO_3$ solution as precursor of silver and *Solanum incanum (L)* EO as reducing agent. Color change from light colorless to dark brown was visually observed after addition of sodium hydroxide (Fig. 5). When the mixtures heated at 60°C, the color changes were more rapid. This color change is due to the Surface Plasmon Resonance (SPR) phenomenon in silver nanoparticles and no further color changes were observed after few minutes, indicating the generation of silver nanoparticles, due to the reduction of silver metal ions Ag^+ into silver nanoparticles Ag^0 via the active molecules present in the *Solanum incanum* EO. This is in line with literature reports [74] and the SPR is indicator of formation of silver nanoparticles by using *Solanum incanum* EO as reducing agent. Syntheses of Fe_3O_4@Ag NC follow two-step process as shown in Fig. 4. The first step of the Fe_3O_4@Ag NC synthesis is the formation of Fe_3O_4 NPs using the essential oil and then addition of silver nitrate and essential oil resulted nanocomposite. Separation of Fe_3O_4 NPs and Fe_3O_4@Ag NC were done with the aid of an external magnet. The possible reaction mechanism of the formation of Fe_3O_4@Ag Nanocomposites in alkaline medium is [75]

$$Ag^+ + F_3O_4 \rightarrow [Ag(F_3O_4)]^+ \quad \text{..... (eq. 4)}$$

$$2[Ag(F_3O_4]^+ + 2OH^- + EO \rightarrow 2Ag + 2F_3O_4 \quad \text{..... (eq. 5)}$$

4.3 Characterization of Synthesized Fe_3O_4 NPs, Ag NPs and Fe_3O_4@Ag NC

4.3.1 UV-Visible Spectrophotometric (UV-Vis) Analysis

UV-Vis spectrophotometer is useful in characterization and can provide certain information about shape, size, and stability of nanoparticles. The plasmonic absorbance phenomenon of nanoparticles makes it detectable by UV-Vis spectrophotometer [76]. UV-Vis absorption spectra of Ag NPs, Fe_3O_4 NPs and Fe_3O_4@Ag NC recorded are shown in Fig.6. The synthesized nanomaterials revealed continuous absorption in the visible range of 200–800 nm with strong absorption peak ~450 nm (red), ~430 nm (blue) and ~350 nm (black) for Ag NPs, Fe_3O_4@Ag NC and Fe_3O_4 NPs, respectively. The position and shape of plasmon absorption are strongly dependent on the particle size, dielectric medium and surface-adsorbed species [77]. According to Bhupendra Chudasama et al only a single SPR band is expected in the absorption spectra of spherical metal nanoparticles, whereas anisotropic particles could give rise to two or more SPR bands depending on the shape of the particles [77]. In our case, a single SPR band is observed in all particles, which leads one to predict that the particles are spherical in shape. Hence, the presence of an SPR band in the spectrum of Fe_3O_4@Ag NC at ~430 nm is an indicative of the formation of a fine layer of silver on the Fe_3O_4 NPs and in agreement with the results obtained from TEM analysis.

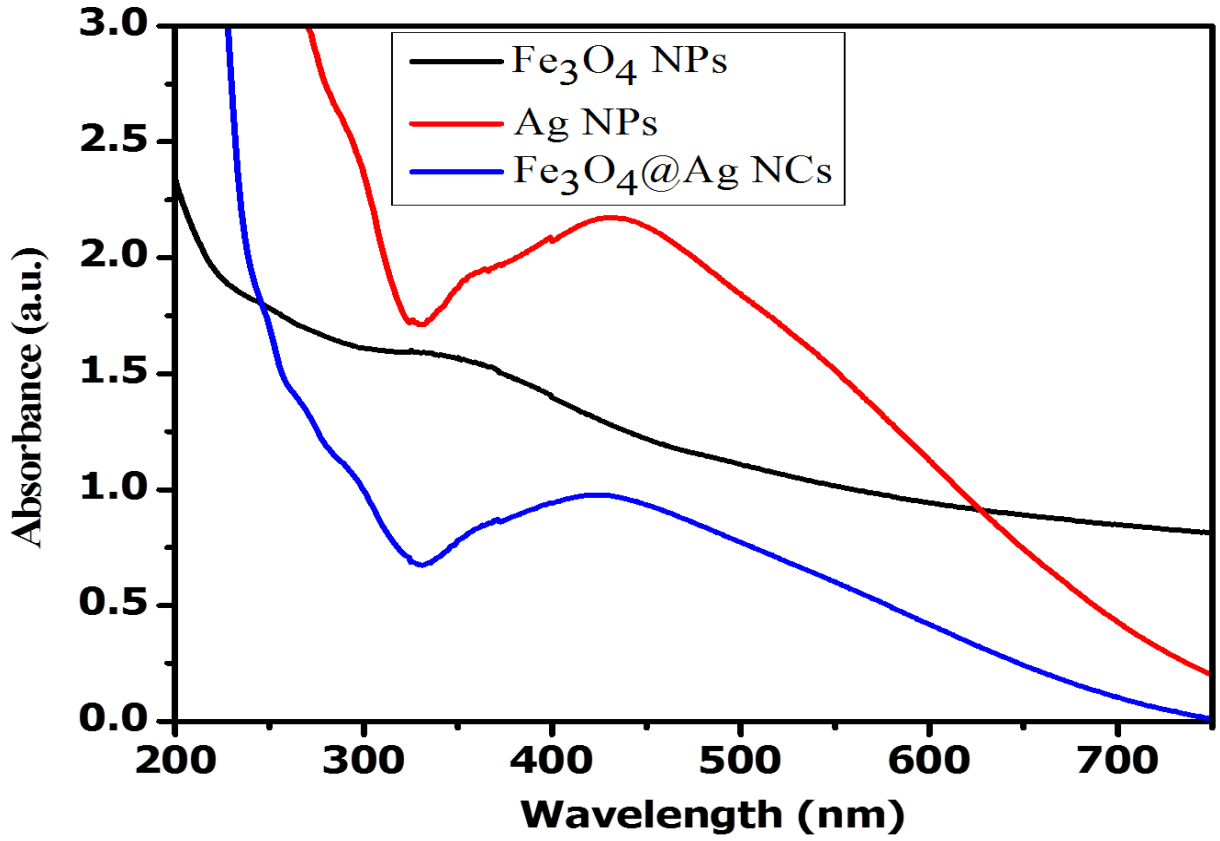

Figure 6: UV-Vis spectra of Fe_3O_4NPs, AgNPs and Fe_3O_4@AgNCs

4.3.2 Fourier Transform Infrared (FTIR) Spectroscopy Analysis

FTIR spectra of Fe_3O_4 NPs, Ag NPs, and Fe_3O_4@Ag NC is shown in Fig.7. The common absorption bands around 3395.8 cm^{-1}, 2923 cm^{-1} and 1416.7 cm^{-1} are indicating characteristic stretching vibration of hydroxyl functional group (O-H), stretching vibration of C-H and bending vibration of O-H on the surface of nanomaterials. The stretching vibration of C=C group also localized at around 1666 cm^{-1}[78]. The presence of these functional groups indicated well capping of essential oil on surface of nanomaterials. The FTIR spectrum exhibit strong bands in the low-frequency region (1000–500 cm^{1}) due to the iron oxide skeleton [79] which is consistent with the magnetite (Fe_3O_4) spectrum [80]. The characteristic band of Fe–O at 570 cm^{-1} was indicative of Fe_3O_4 NPs.

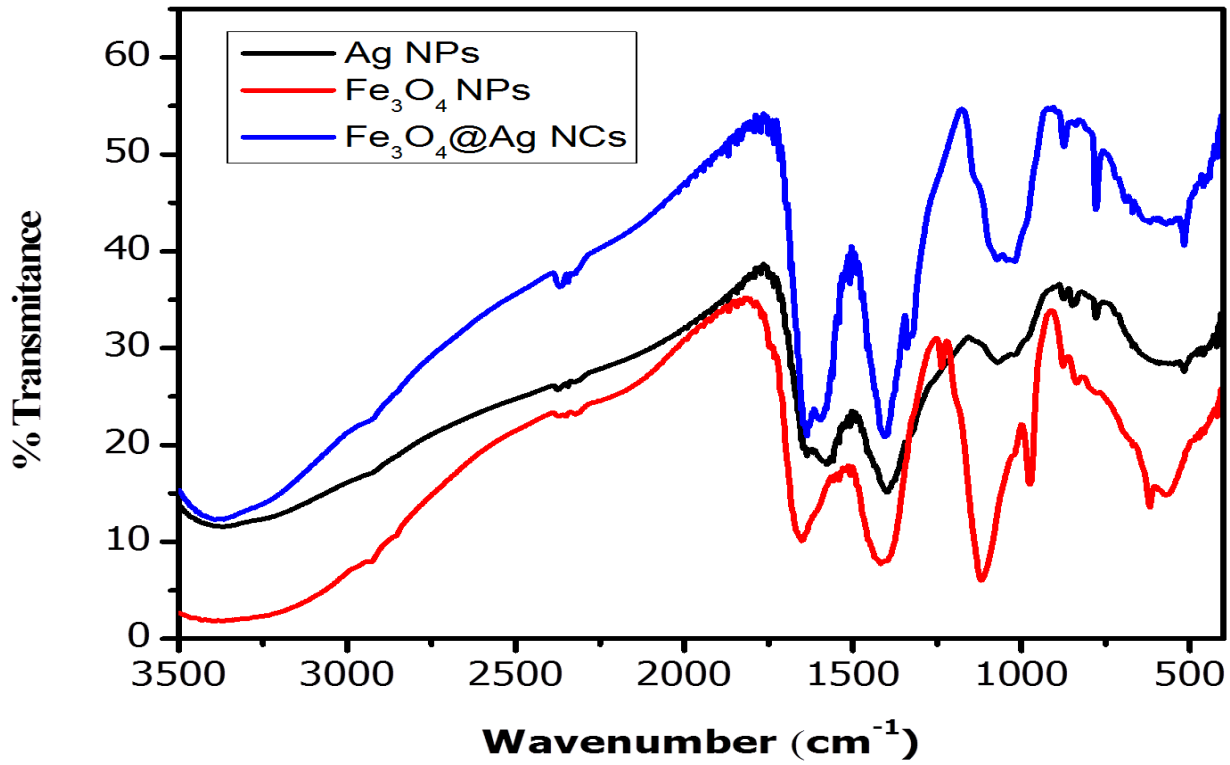

Figure 7: FTIR spectra of Ag NPs, Fe_3O_4 NPs and Fe_3O_4@Ag NCs

4.3.4 X-ray Diffraction (XRD) Pattern Analysis

The phase purity and crystallinity of the prepared Fe_3O_4NPs, AgNPs, and Fe_3O_4@AgNC were examined by X-ray diffraction technique (XRD) (Fig. 11). The XRD pattern indicates that the product mostly consists of magnetite in Fe_3O_4 NPs peaks, Ag in AgNPs peaks and Magnetite and Ag in Fe_3O_4@Ag NC peaks. Peaks at 2θ values of 30.36º, 35.7º, 43.357º, 53.59º, 57.209º and 62.34º corresponding to (hkl), (220), (311), (400), (422), (511) and (404) Bragg's reflections for Fe_3O_4 NPs which is similar to that reported before for Fe_3O_4 nanoparticles by [81, 82]. Ag NPs shows diffraction peaks at 2θ values of 38.074, 44.365, 64.485, and 77.424 corresponding to (hkl) values of (111), (200), (220) and (311) Bragg's reflections.

XRD spectrum with the standard XRD data for magnetite (JCPDS file No. 96-900-6248) and for silver (JCPDS file No 096-901-2432) clearly illustrates that both Fe_3O_4NPs and AgNPs synthesized with crystal structure cubic (space group Fm-3m (227) and crystal structure cubic (space group Fm-3m-225), respectively. The XRD patterns of Fe_3O_4 NPs and Fe_3O_4@Ag NC were similar within the limits of error; the only difference between them was the presence of weak

peak at 38.134 (2θ values) in the spectrum of the Fe_3O_4@Ag NC (Fig. 11). Therefore, those peaks indicate the successful formation of the Fe_3O_4@Ag nanocomposite. The average crystalline size of the nanomaterials can be obtained from Scherrer equation [83]:

$$d = \frac{K\lambda}{\beta \cos\theta} \quad \text{..... (eq. 6)}$$

Where d is particle diameter, k is constant, λ is wavelength of the Cu-Kα irradiation, β is the peak width of half-maximum, and θ is diffraction angle. The Full Width at Half Maximum (FWHM) values were used to calculate the size of the nanoparticles. The average size of silver nanoparticles synthesized from *Solanum incanum* EO was calculated using Scherer's equation from the above Scherer's constant value k= 0.94. The average crystalline size is calculated for Fe_3O_4 NPs, Ag NPs, and Fe_3O_4@Ag NC to be about 33 nm, 21 nm and 14.8 nm, respectively.

The calculated lattice constant for magnetite shown in Table 6 is in good agreement with standard lattice parameter a=8.39Å [84]. For Ag also the calculated lattice constant is in good agreement with the reported value and the sample exhibits smaller cell volumes. Earlier workers reported similar results for Ag nanoparticles [83]. Generally, XRD results clearly show that the Fe_3O_4 NPs, Ag NPs, and Fe_3O_4@Ag NC were successfully synthesized with the help of essential oil of *solanum incanum(L)* root as reducing and capping agent.

Table 3: The variation of crystalline size, lattice parameter value of biosynthesized Fe_3O_4 NPs

peak position (2θ)	FWHM	size of the nanoparticle (nm)	Average size (nm)	d-spacing (nm)	Lattice Parameter, a (Å)	hkl
30.33	0.32	30.21	27.86	2.95042	8.34505	220
35.66	0.48	34.52		2.51416	8.33853	311
43.3	0.28	31.52		2.08359	8.33437	400
53	0.84	19.73		1.4794	8.34334	422
57.38	0.28	32.22		1.60519	8.3408	511
63.02	0.44	18.945		1.4754	8.34612	404

Table 4: The variation of crystalline size, lattice parameter value of biosynthesized Ag NPs

peak position (2θ)	FWHM	size of the nanoparticle (nm)	Average size (nm)	d-spacing (nm)	Lattice parameter, a (Å)	hkl
38.1	0.3600	23.6	21.76	2.3608	4.089	111
44.3	0.600	14		2.0452	4.0904	200
64.48	0.600	20.36		1.4455	4.0885	220
77.38	0.5200	29.12		1.2325	4.0877	311

Table 5: The variation of crystalline size, lattice parameter value of biosynthesized Ag NPs

peak position (2θ)	FWHM	size of the nanoparticle (nm)	Average size (nm)	d-spacing (nm)	Lattice Parameter, a (Å)	hkl
30.36	0.36	23.1	14.8	2.9442	8.34505	220
35.88	0.56	14.8		2.5031	8.33853	311
43.46	0.24	34.6		2.0823	8.33437	400
53.40	0.52	15.93		1.7158	8.34334	422
57.64	0.36	23		1.5993	8.3408	511
63.18	0.72	11.54		1.4717	8.34612	404
38.45	0.04	4		2.2967	4.33	111

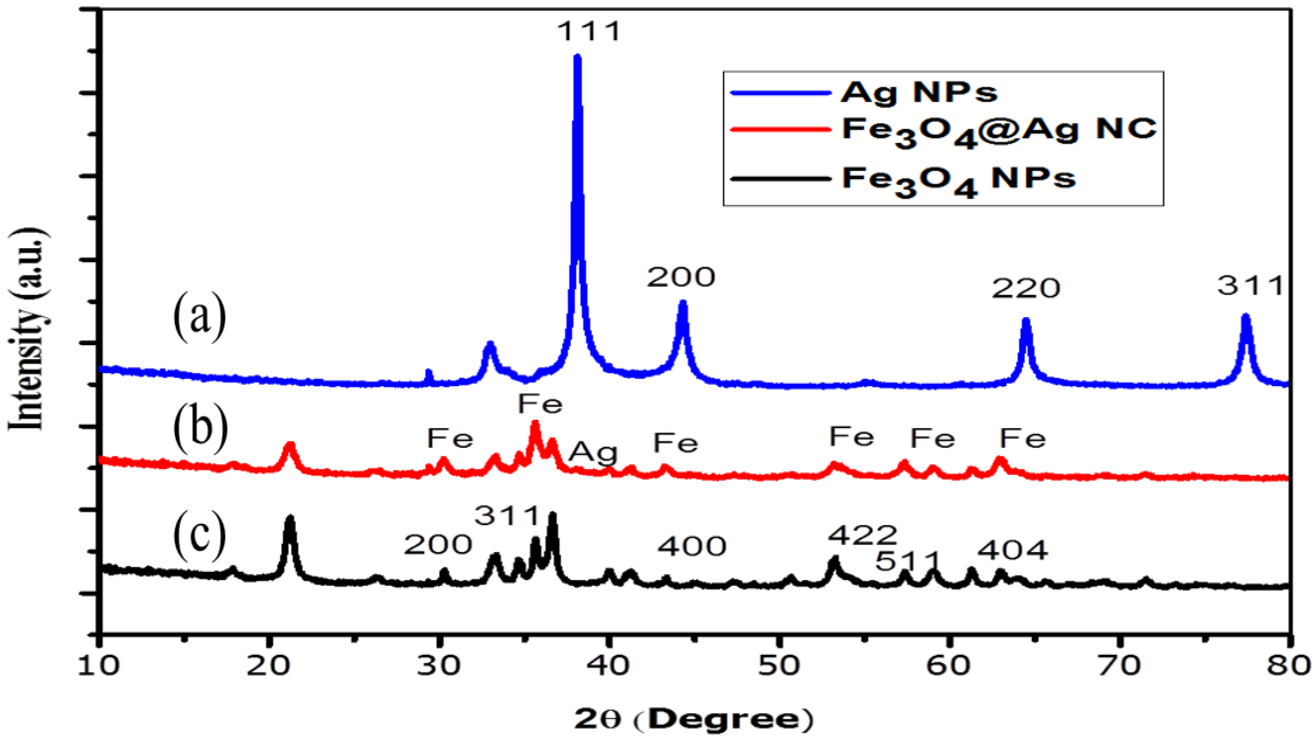

Figure 8: XRD patterns of Fe_3O_4 NPs (a), Ag NPs (b) and Fe_3O_4@Ag NC (c)

4.3.3 Scanning Electron Microscope (SEM) and Energy Dispersive X-ray (EDX) Analysis

Scanning electron microscopy technique was employed to study morphology of synthesized Fe_3O_4 NPs, Ag NPs, and Fe_3O_4@Ag NC. SEM image of Fe_3O_4 NPs (Fig. 8a &b), Ag NPs (Fig. 9a & b) and Ag@Fe_3O_4 NC (Fig. 10a &b) show that the morphology of the synthesized nanomaterials is higher polydispersity of Fe_3O_4@Ag NC than Fe_3O_4 NP and Ag NPs.

In order to confirm the formation of (Ag NPs, Fe_3O_4 NPs, and Ag@Fe_3O_4 NC), EDX analysis was performed. During the EDX measurement different areas were focused and corresponding peaks are shown in figure 8(c), 9(c) and 10(c). In the EDX of synthesized Ag nanoparticle, Ag can be seen, which confirm the formation of Ag NPs, in the EDX of synthesized Fe_3O_4 NPs, Fe and O can be seen which confirm formation of Fe_3O_4 NPs and in Fe_3O_4@Ag NC EDX spectrum, Ag, Fe, and O can be seen which confirm formation of Fe_3O_4@Ag NC. Fe_3O_4 NPs EDX spectrum Fig. (8(c)) shows the quantity of Fe and O were 64.38 % and 33.60%, respectively, while in Ag NPs EDX spectrum (Fig.9(c)) the values of Ag were 90.64% and in Fe_3O_4@Ag NC EDX spectrum (Fig.10 (c)) quantity of Fe, O and Ag were 42.76%, 47.67% and 2.06%, respectively. Details of the three

EDX spectra of the Ag NPs, Fe_3O_4 NPs, and Fe_3O_4@Ag NC values measured in apparent concentration and %weight are listed in Table 3.

Table 6: EDX spectrum of Fe_3O_4 NPs (a) Ag NPs (b) Fe_3O_4@Ag NC (c)

Element	EDX of Fe_3O_4 NPs		EDX of Ag NPs		EDX of Fe_3O_4@Ag NC	
	%Weight	Apparent concentration	%Weight	Apparent concentration	Weight %	Apparent con centration
Fe	64.38	25.67			42.76	12.35
O	33.60	30.64	7.24	1.93	47.67	29.07
Ag	-	-	90.64	48.50	2.06	0.55
C	-	-	1.43	0.6	6.12	0.70
N	0.91	0.76	0.69	0.37	1.39	1.13
S	1.05	0.45	-	-	-	-
Si	0.08	0.21	-	-	-	-

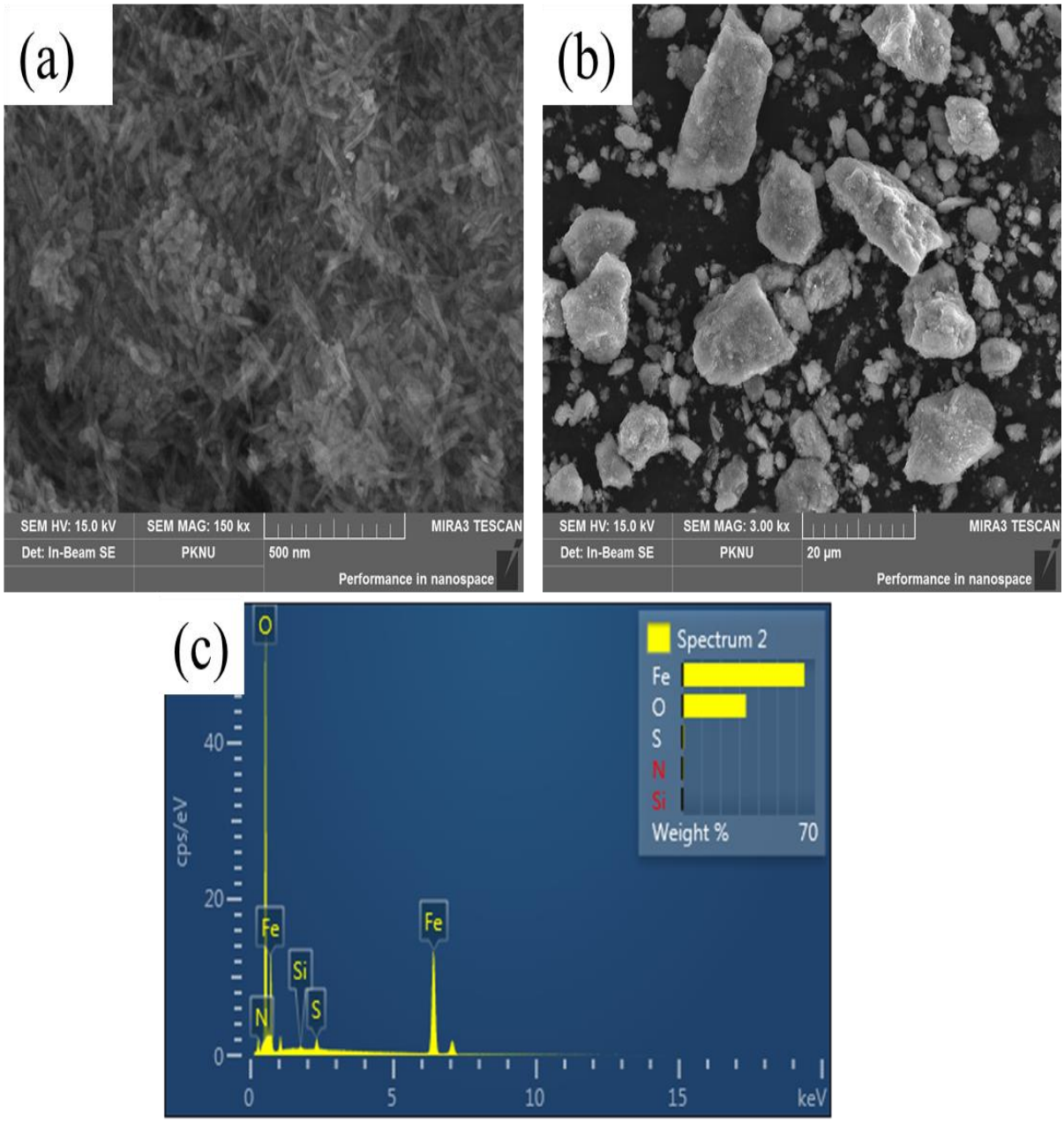

Figure 9: SEM images of Fe_3O_4 NPs powder (a & b) and its EDX spectrum(c)

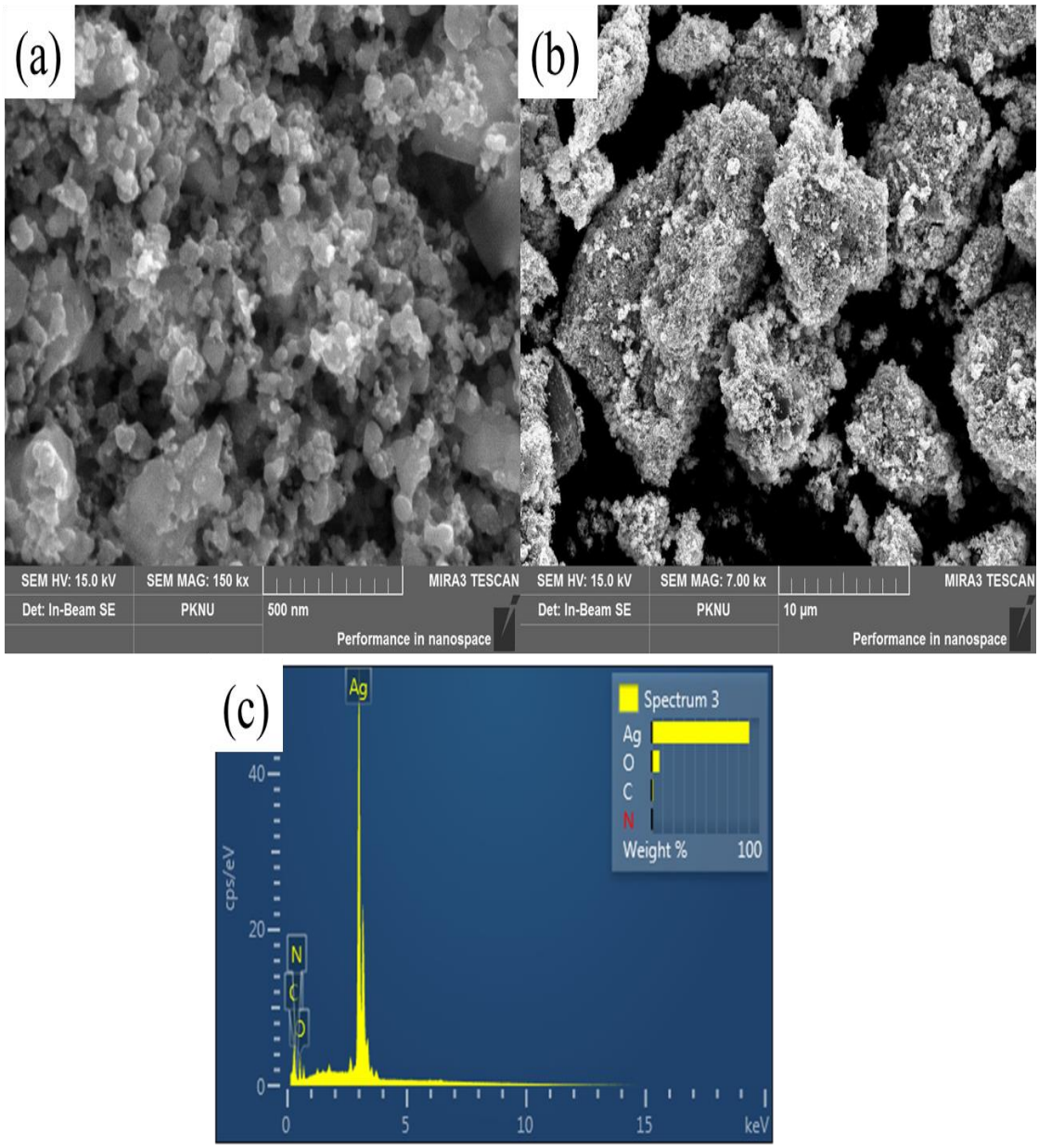

Figure 10: SEM images of Ag NPs powder (a & b) and its EDX spectrum (c)

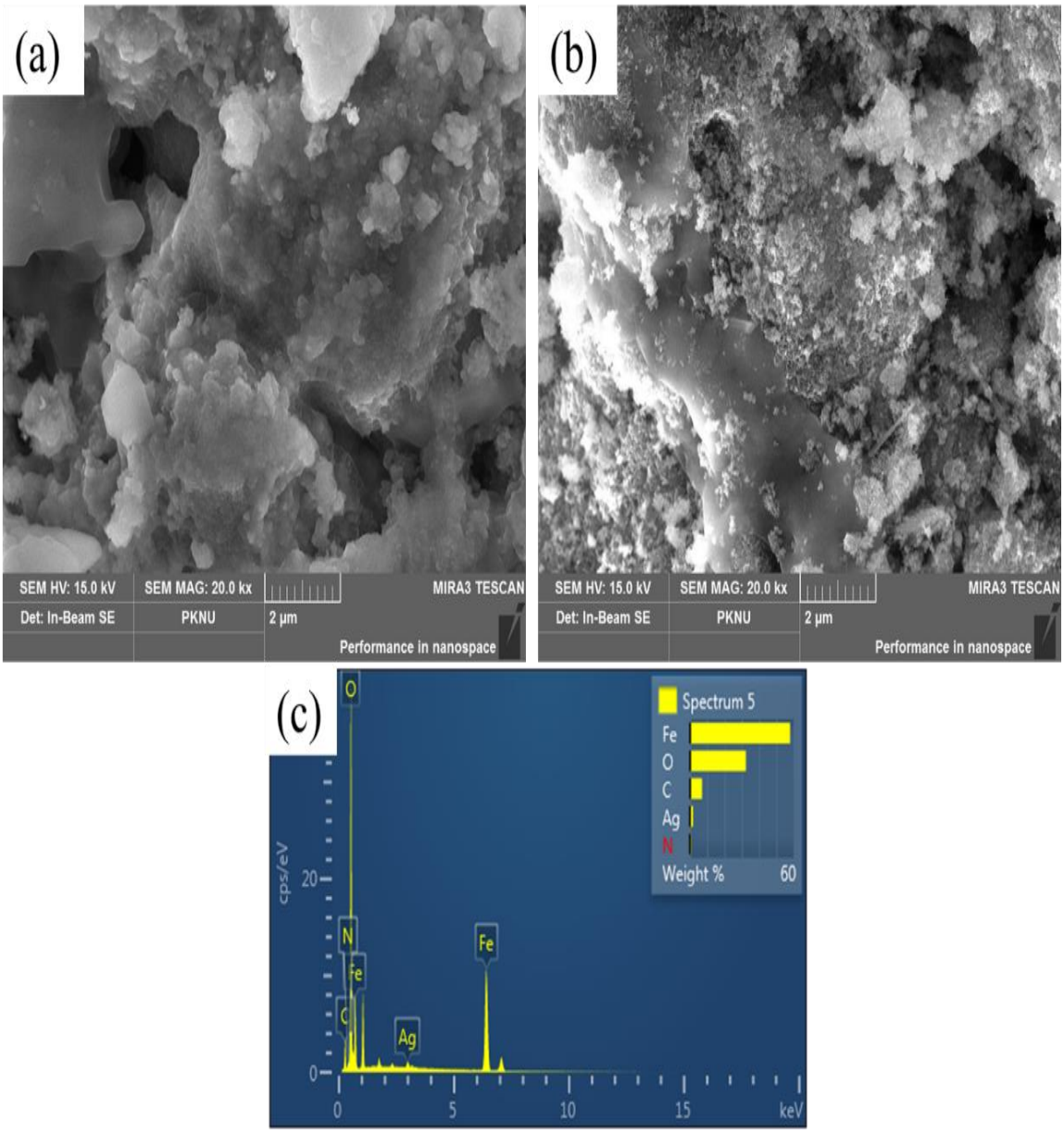

Figure 11: SEM images of Fe_3O_4@Ag NC powder (a & b) and its EDX-Spectrum (c)

4.3.5 Transmission Electron Microscope (TEM) Analysis

Fig. 12 shows the representative TEM micrograph of the EO mediated synthesized Ag NPs at different magnification scales. As it is shown in the Fig. 12 (a-c), the prepared Ag NPs have spherical structure. Fig. 12d shows the selected area electron diffraction (SAED) of Ag NPs is attributed to the high crystallinity of the nanomaterial. The average particle size of the as synthesized Ag NPs calculated from TEM image is 23 nm.

Fig. 13 shows the representative TEM micrograph of the EO mediated synthesized Fe_3O_4 NPs at

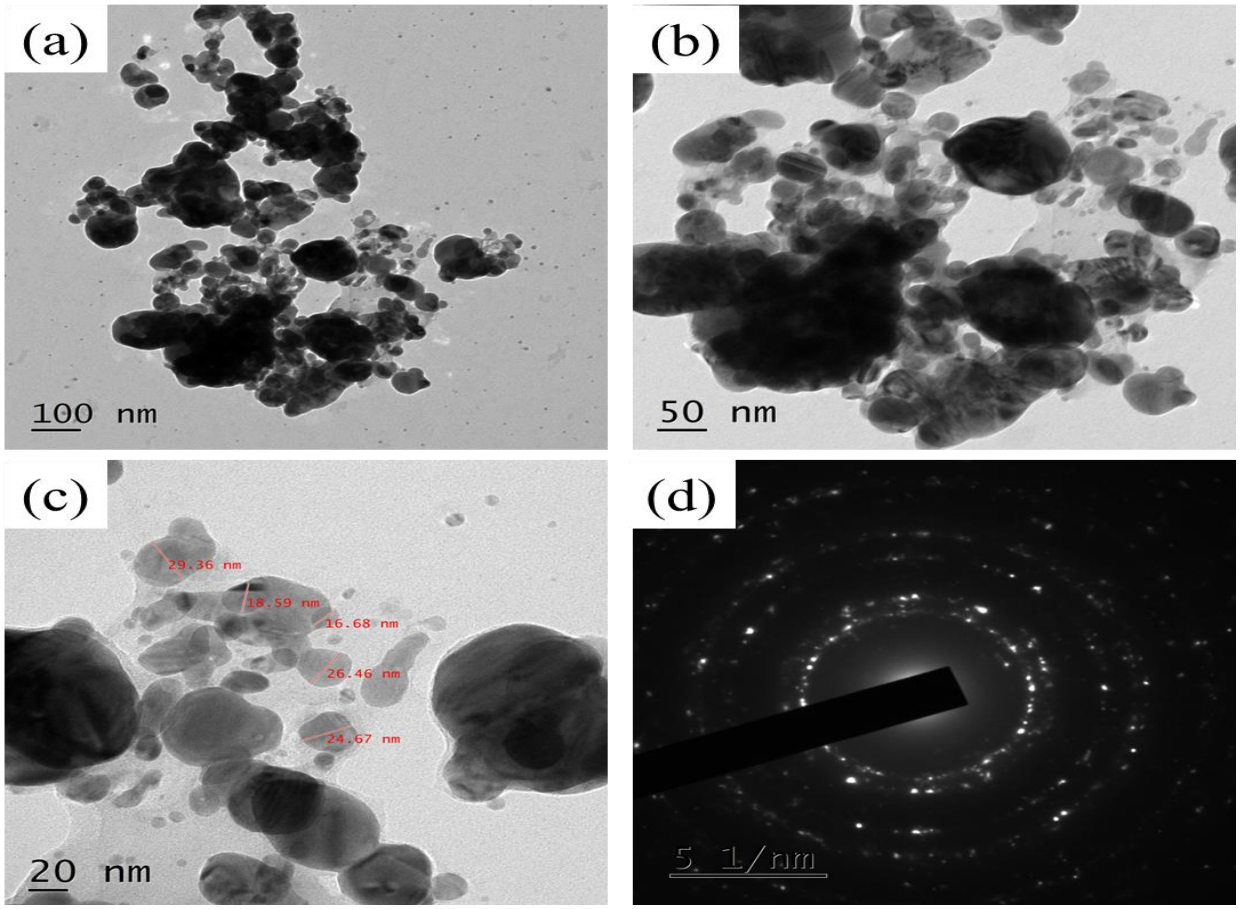

different magnification scales. Fig. 13d shows the selected area electron diffraction (SAED) of Fe_3O_4 NPs is attributed to the high crystallinity of the nanomaterial. The average particle size of the synthesized Fe_3O_4 NPs calculated from TEM image is 11 nm.

Figure 12: TEM images at 100 nm (a), 50 nm (b), 20 nm (c) magnification scale and selected area electron diffraction (SAED) of silver nanoparticles (Ag NPs) (d).

Fig. 14 shows the representative TEM images of the synthesized Fe_3O_4@Ag NC at different magnification scales. As it is shown in the Fig. 14 a-c, the prepared NC have spherical structure. Fig. 14d shows the selected area electron diffraction (SAED) of Fe_3O_4@Ag NC is attributed to the high crystallinity of the synthesized Fe_3O_4@Ag NC. The average particle size of the as synthesized Fe_3O_4@Ag NC calculated from TEM image is 11 nm.

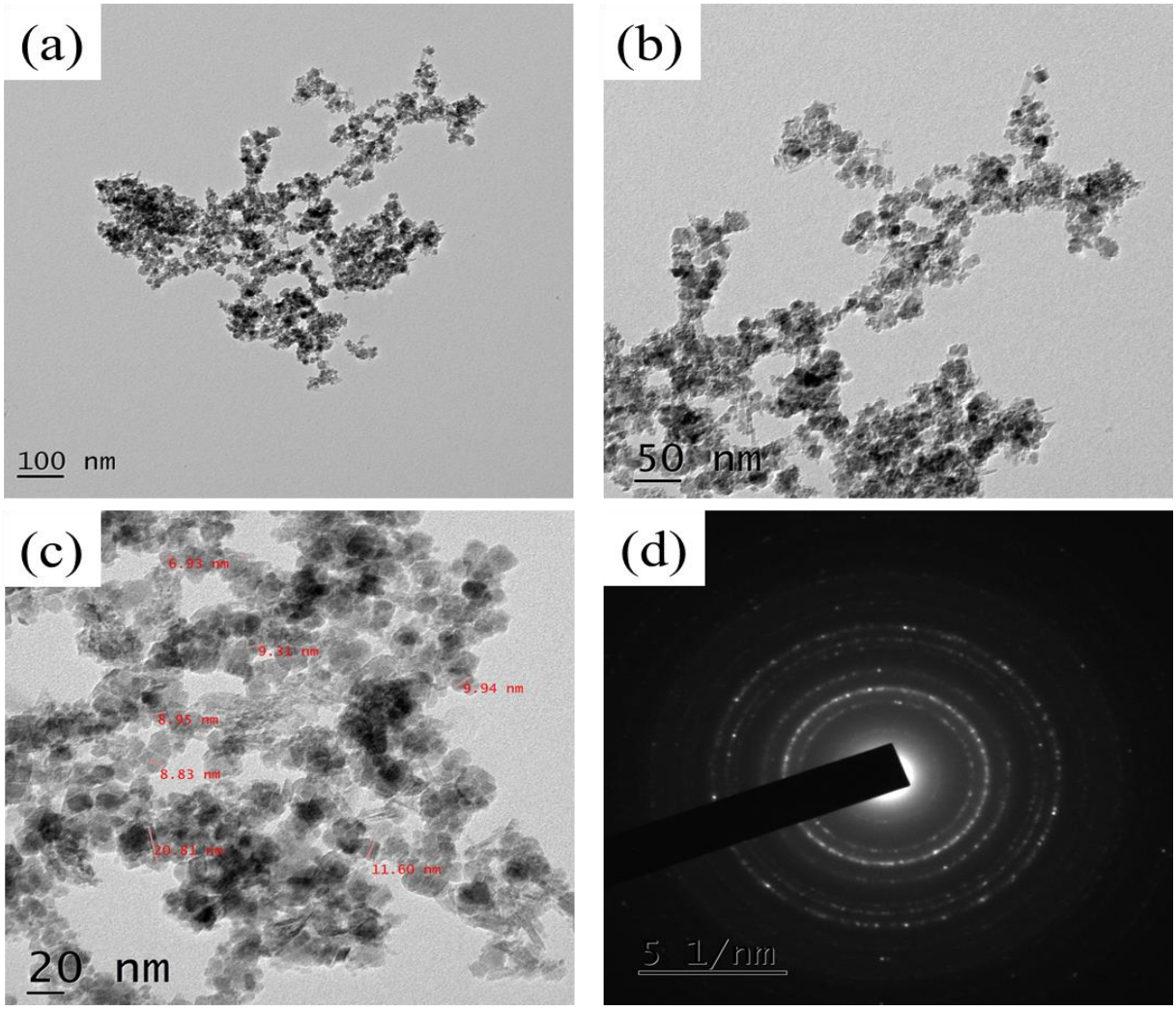

Figure 13:TEM images at 100 nm (a), 50 nm (b), 20 nm (c) magnification scale and selected area electron diffraction (SAED) of magnetite nanoparticles (Fe_3O_4 NPs) (d).

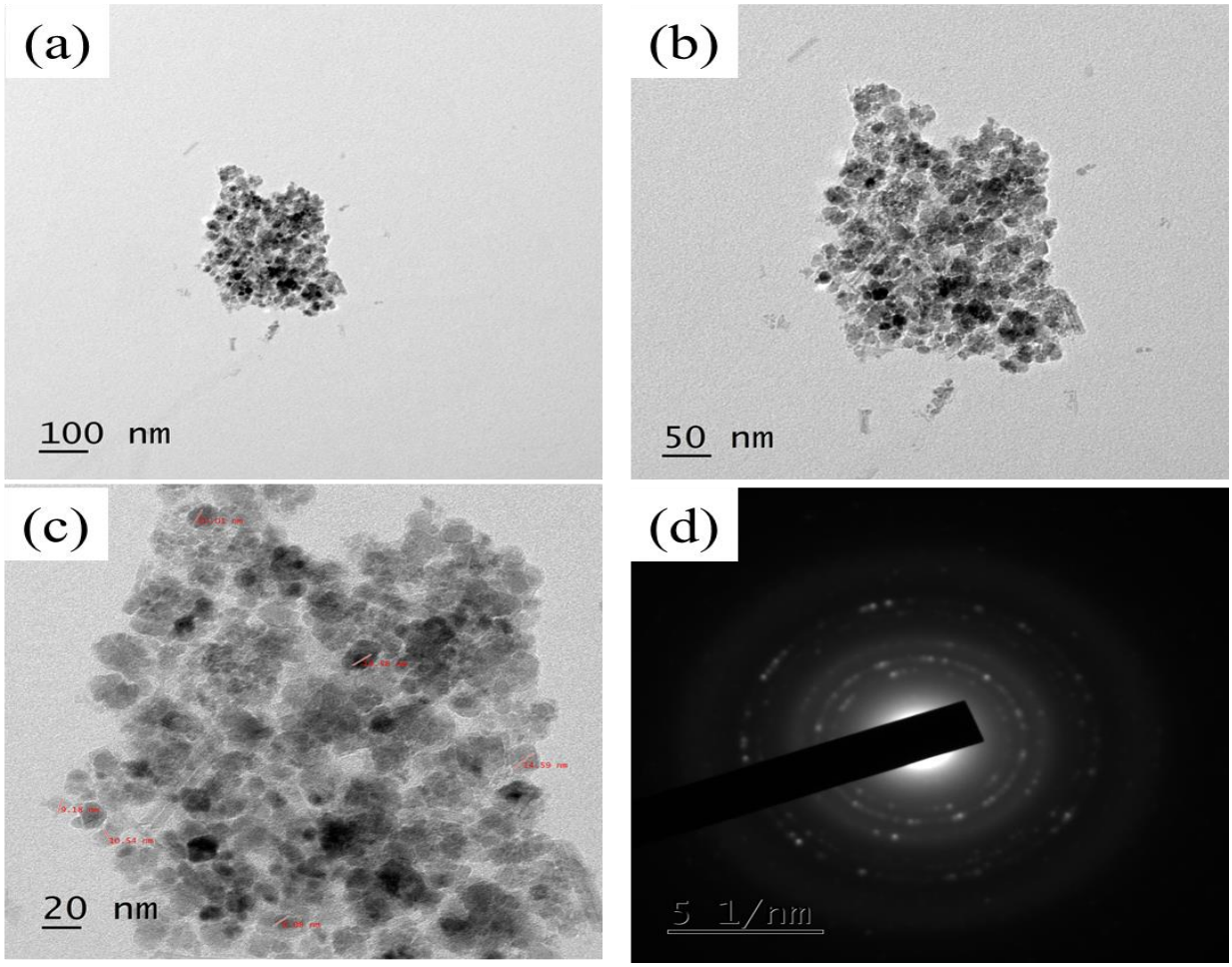

Figure 14:TEM images at 100 nm (a), 50 nm (b), 20 nm (c), magnification scale and selected area electron diffraction (SAED) of Fe_3O_4@Ag NC (d).

4.4 Application of Synthesized Fe_3O_4 NPs, Ag NPs, And Fe_3O_4@Ag NC

4.4.1 Adsorption of MB dye on to Fe_3O_4 NPs

Synthesized Fe_3O_4 NPs was used to remove MB dye from water through adsorption process. Adsorption parameters were optimized by considering only initial concentration of MB dye and adsorbent dosage (Fe_3O_4 NPs) by maintaining room temperature and pH 11 at time interval of 20 minutes until 120 minutes. Maximum adsorbance of 91.72% was obtained at 100 min starting with $4x10^{-4}$M MB dye solution and using 40 mg of adsorbent (Fig.15).

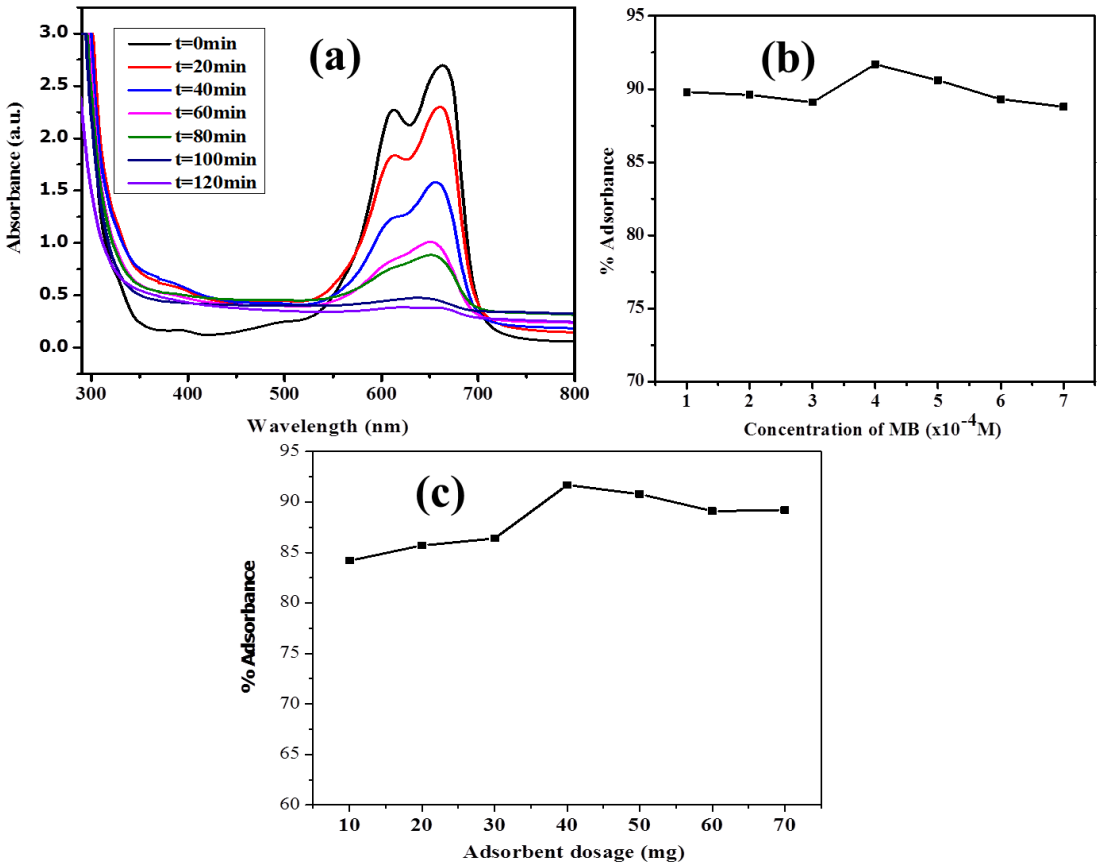

Figure 15: UV-Vis absorption spectra of MB at different time interval of adsorbance (a), concentration effect of MB (b), and effect of adsorbent dosage (Fe_3O_4 NPs) (c).

4.4.3 Kinetic Study

The rate of reaction in the photodegradation experiment was evaluated using pseudo-first order and pseudo-second order kinetics model [85]. Pseudo-first order kinetic model equation is given as

$$q_e - q_t = \log q_e + \frac{K_1 t}{2.303} \quad \text{(eq.7)}$$

Where, q_e(mg/g) is the amount MB decomposed at equilibrium time; q_t (mg /g) is amount of MB decomposed at time, t; and K_1 (min^{-1}) is the rate constant of the pseudo-first-order kinetic model. The values of K_1 were calculated from the slope of linear plots of log (q_e-q_t) versus t [86-88].

The pseudo-second-order equation [85]:

$$\frac{t}{q_t} = \frac{1}{k_2 q_e^2} + \frac{1}{q_e} t \quad \text{..... (eq. 8)}$$

where, q_e (mg/g) is the amount of MB decomposed at equilibrium time; q_t (mg /g) is amount of MB decomposed at time, t; and K_2 (min^{-1}) is the rate constant of the pseudo second order kinetic model. The fig. 17 shows that the adsorption removal follows perfectly the pseudo-second-order kinetics, and the fairness of the fit is indicated by the linear regression value, R^2 = 0.934 for Fe_3O_4 NP it implies that 'Chemisorption' took place during the adsorption process.

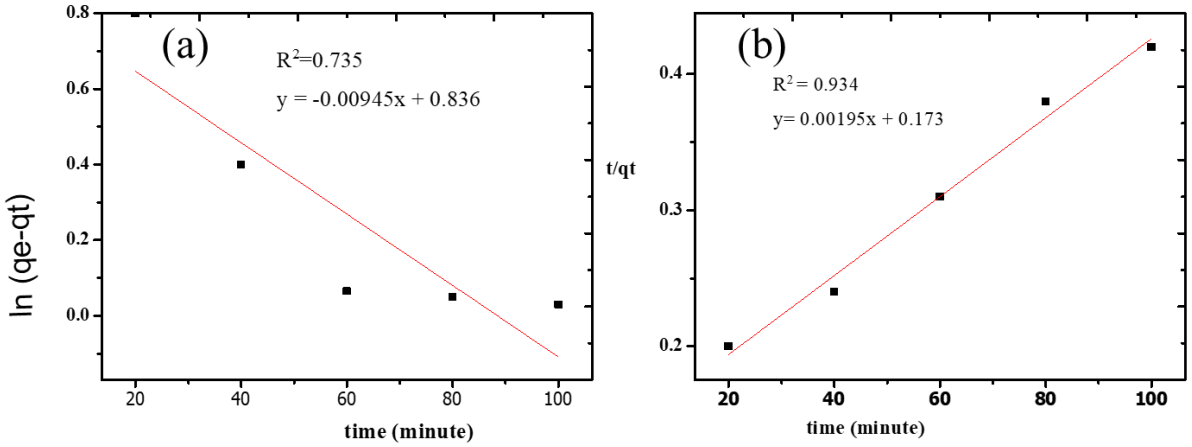

Figure 16: Pseudo first order kinetics model of methylene blue using Fe_3O_4 NPs (a) and (b) and pseudo second order kinetics model of methylene blue using Fe_3O_4 NP

Table 7: Pseudo-first order and pseudo-second order kinetic model values

Catalyst	Pseudo first order		Pseudo second order	
	K_1	R^2	K_2	R^2
Fe_3O_4 NPs	-0.00945	0.735	0.00195	0.934

4.4.2. Photodegradation of MB Dye Fe_3O_4@Ag NC and Ag NP

The photodegradation experiment was performed by adding 40 mg of catalyst and 3 drops of 30% H_2O_2 solution to 100 mL of the dye solution (4×10^{-4} M). The suspension was magnetically stirred in the dark for 30 minutes in order to attain adsorption-desorption equilibrium before the irradiation by UV light. The main advantage of using the UV light was to produce electron and hole pair (e^-/h^+) with high energy state that migrate to the nanoparticle surface and initiate a wide range of chemical reactions [72]. It was observed that the intense blue color of the initial solution disappears gradually and becomes colorless as the irradiation time increases, indicating the degradation of the dye under UV light irradiation, as can be seen in Fig. 16. From the Fig.16 it can be seen that the absorption spectrum maximum of MB steadily decreases as the exposure time of UV light increases from 0 to 120 min, indicating the process of photodecomposition of the dye.

The photocatalytic activities of the naked silver nanoparticles and a solution without the photocatalyst in presence of H_2O_2 solution, for comparison, were also investigated. It was found that, without adding the photocatalyst, the degradation of MB was very slow at only 2% after 120 min, while the Ag NPs showed lower photocatalytic degradation of about 90.7%. The color removal process of MB using Fe_3O_4@AgNC was significantly higher, reaching almost 98.1% degradation. Further, Fe_3O_4@Ag NC has advantage over Ag NPs that it can easily separate from solution after photodegradation using external magnet.

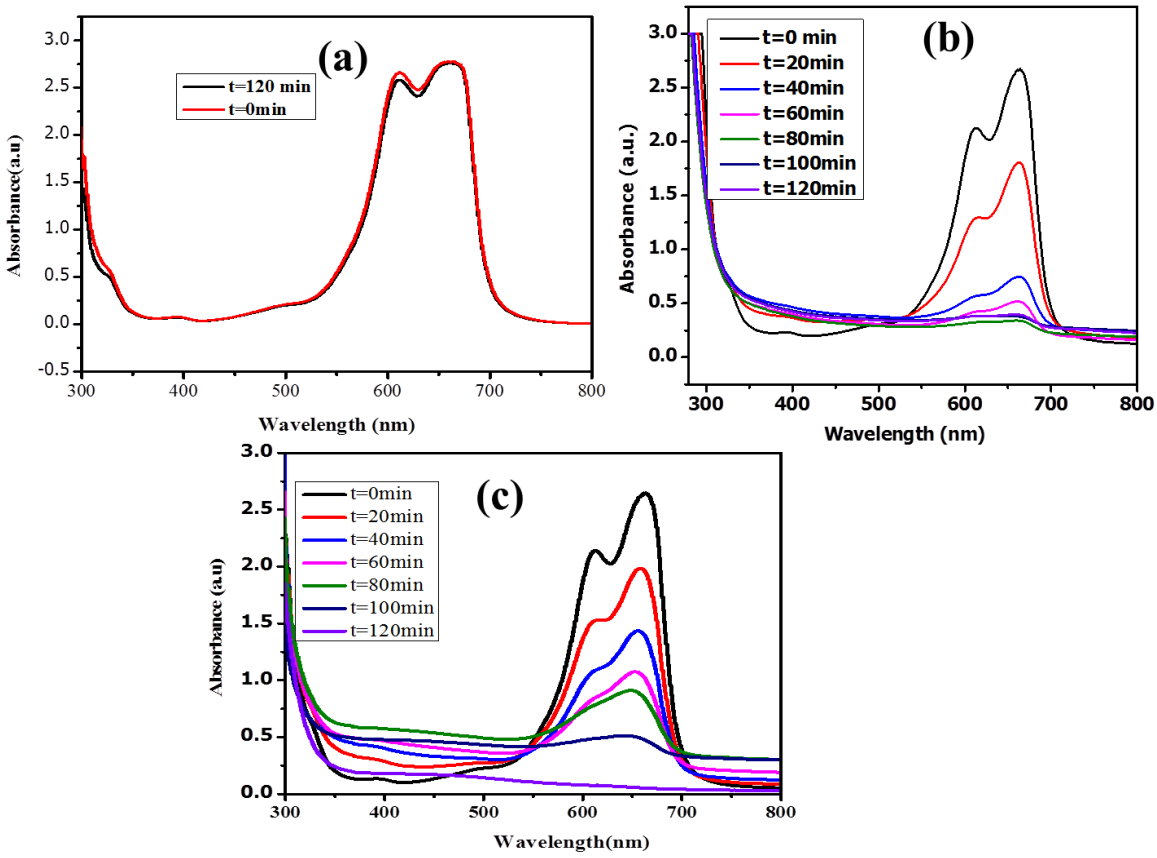

Figure 17: UV–Vis absorption spectra for photodegradation of MB using H_2O_2 (a), Ag NPs (b), and Fe_3O_4@Ag NC (c).

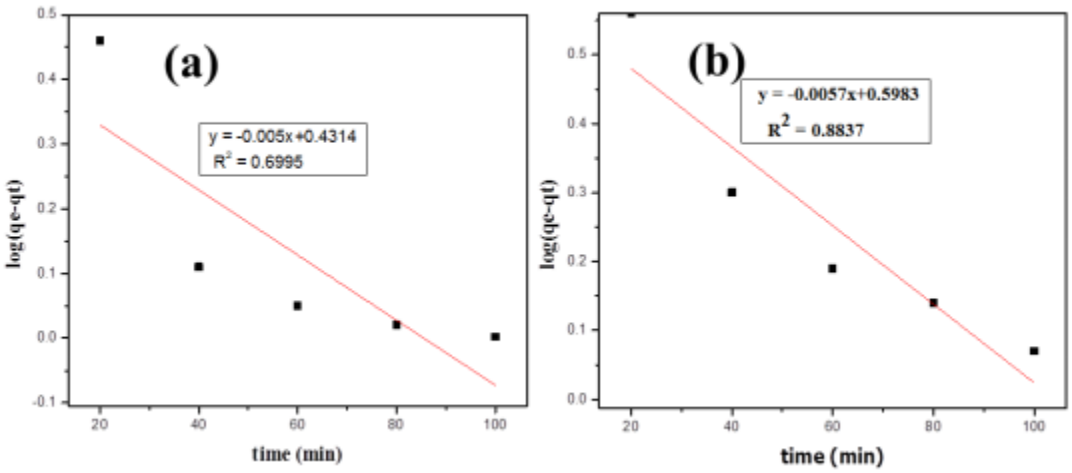

Figure 18: Pseudo first order kinetics model of MB using Ag NPs (a) and Fe_3O_4@Ag NC

Table 8: Pseudo-first order and pseudo-second order kinetic model values

Catalyst	Pseudo first order		Pseudo second order	
	K_1	R^2	K_2	R^2
Ag NPs	-0.005	0.6995	0.0025	0.9241
Fe_3O_4@Ag NC	-0.0057	0.8837	0.0019	0.9683

4.4.4 Recyclability of Fe_3O_4@Ag NC for Methylene Blue

The reusability of Fe_3O_4@Ag NC was studied in order to see the cost effectiveness of the method. This was performed in a very simple way that after the degradation of MB dye, the Fe_3O_4@Ag NC were separated easily from the solution using an external magnet, while the supernatant was decanted. Then, the magnetic nanomaterial was washed with distilled water and reused for degradation with a fresh lot of MB solution. As can be seen in Fig.18 and Table 9, after using the Fe_3O_4@Ag NC for five times, the photodegradation of MB did not show any significant loss of activity. These results confirmed that the Fe_3O_4@Ag NC are not photo-corroded during photocatalytic oxidation of the dye.

Table 9 : Recyclability of Fe_3O_4@Ag NC

cycle	% degradation over time						
	t=0 min	t=20 min	t=40min	t= 60min	t= 80min	t =100 min	t= 120min
Cycle 1	0	25.8	40	60.7	66	87	96.7
Cycle 2	0	23.7	39	59	64.45	84	95.23
Cycle 3	0	22	37.94	58.3	61	80	89
Cycle 4	0	20	34.33	53	60.43	76	84
Cycle 4	0	18	30	52	60	70	78.9

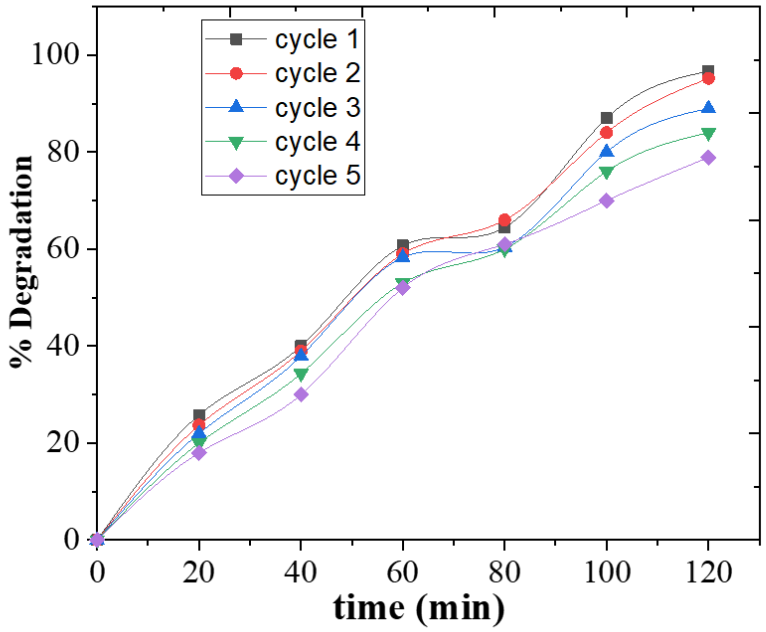

Figure 19: Recyclability of Fe_3O_4@Ag NC

4.4.5 Antibacterial Activity

In this study, *Solanum incanum (L)* essential oil mediated synthesized Fe_3O_4@Ag NC, Fe_3O_4 NPs, Ag NPs at concentrations of 25µg/ml, 50µg/ml and 75µg/ml were tested for antibacterial activity using gram negative and gram-positive bacteria strains of *Escherichia coli* and *Staphylococcus aureus* using disc diffusion method. (Table 9 and Fig. 13) show the results of antibacterial activities of synthesized Fe_3O_4@Ag NC, Fe_3O_4 NPs, AgNPs evaluated from the well diffusion method. Results showed that synthesized Fe_3O_4@AgNC, Fe_3O_4 NPs, Ag NPs have significant antimicrobial activity against the tested pathogenic bacteria. The result indicated that Fe_3O_4@Ag NC has higher Antibacterial activity advantage than Fe_3O_4 NPs and Ag NPs. All synthesized particles tested for antibacterial activity showed high activity against *S. aureus* bacteria when compared to E. coli. The different sensitivities of gram positive and gram-negative bacteria could be explained in accordance with the morphological differences between these microorganisms, due to different polarities of their cell membrane. Smaller negative charge S. aureus membrane than *E. coli*. This would allow a higher level of penetration of negatively charged free radicals such as, superoxide

radical anions and peroxide ions, causing *S. aureus* damage and cell death at lower concentrations than those required to damage *E. coli*. Besides gram negative bacteria has an outer polysaccharide membrane carrying the structural lipopolysaccharide components, and this makes the cell wall impermeable to lipophilic solutes. The gram positive stains should be more susceptible having only an outer peptidoglycan layer which is not an effective permeability barrier [89].

Table 10: Antibacterial activity of synthesized Ag NPs

Microorganism	Zone of Inhibition of Ag NPs (mm)			
	25µg/mL	50 µg/mL	75µg/mL	+ve control
Staphylococcus aureus	15	18	19	24
Escherichia coli	9	10	12	14

Table 11: Antibacterial activity of synthesized Fe_3O_4 NPs

Microorganism	Zone of Inhibition of Fe_3O_4 NPs (mm)			
	25µg/mL	50 µg/mL	75µg/mL	+ve control
Staphylococcus aureus	10	15	17	20
Escherichia coli	7	7	8	12

Table 12: Antibacterial activity of synthesized Fe_3O_4@Ag NC

Microorganism	Zone of Inhibition of Fe_3O_4@Ag NC (mm)			
	25µg/mL	50 µg/mL	75µg/mL	+ve control
Staphylococcus aureus	15	17	23	25
Escherichia coli	14	15	15	20

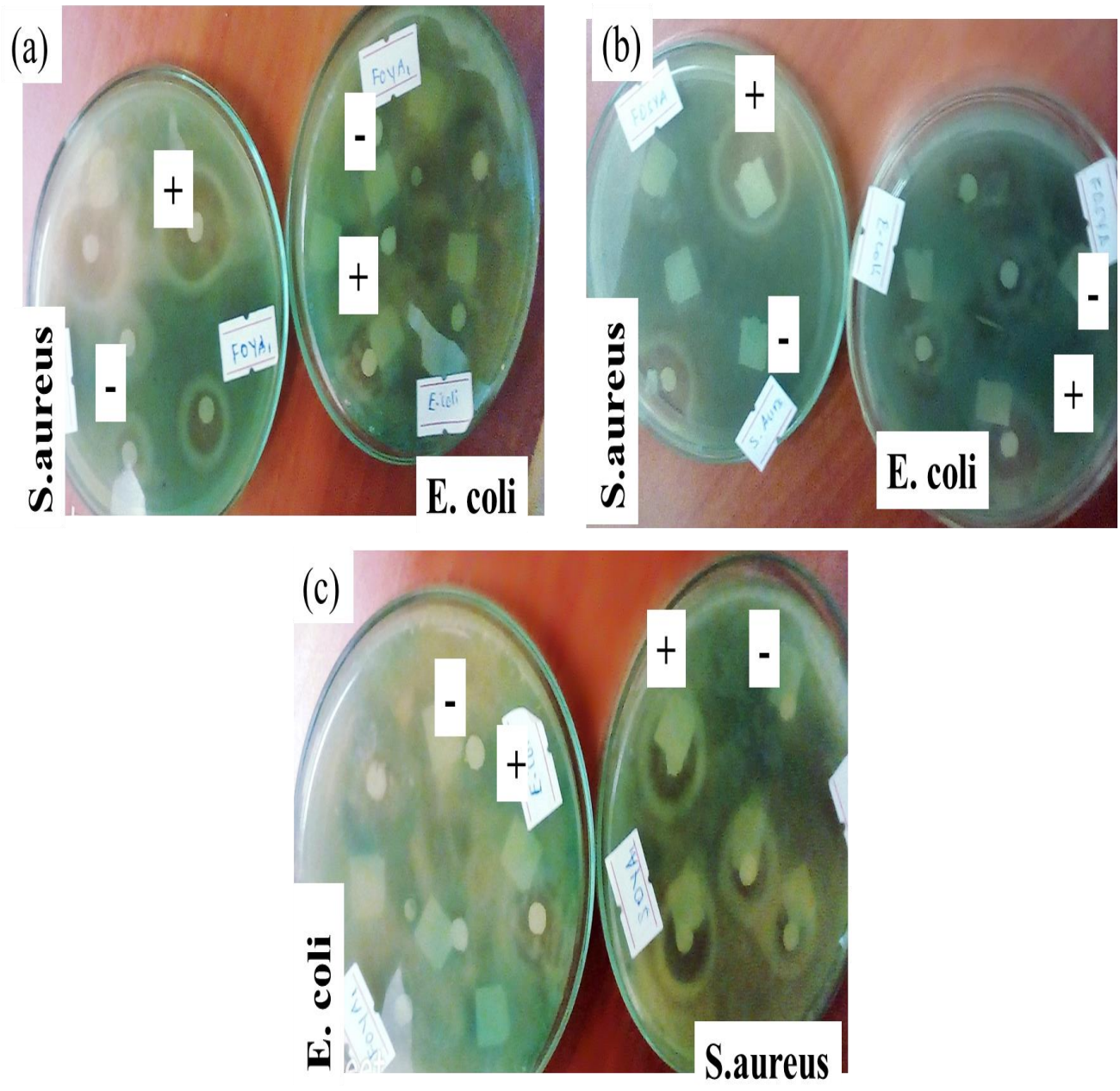

Figure 20: Antibacterial activity Zone of inhibition of synthesized Fe_3O_4@Ag NC (b), Fe_3O_4 NPs (a), Ag NPs (c)

Chapter Five

5 Conclusion and Recommendation

5.1 Conclusion

In this study, Fe_3O_4 NPs, Ag NPs and Fe_3O_4@Ag NC have been synthesized successfully via a simple and cost-effective green method using essential oil of *Solanum incanum (L)*. It can act as both a reducing agent and capping agent. The Fe_3O_4 NPs, Ag NPs and Fe_3O_4@Ag NC were characterized by UV–Vis, FTIR, XRD, FESEM, EDAX and TEM analysis. Adsorption study of methylene blue (MB) using Fe_3O_4 NPs was done and maximum removal efficiency of 91.72% was obtained. Photodegradation study of MB dye solution was done using Ag NPs and Fe_3O_4@Ag NC and maximum removal efficiency of 90.7% and 98.1% respectively were obtained for Ag NPs and Fe_3O_4@Ag NC. The result indicated that Fe_3O_4@Ag NC has higher degradation efficiency (98.1%) and reusability advantage than Ag NPs (90.7%). Adsorption Kinetic study showed that the catalyst best fit to Pseudo second order than pseudo first order kinetic model. The biosynthesized Fe_3O_4 NPs Ag NPs and Fe_3O_4@Ag NC were found to have a high antibacterial activity against *S. aureus* than *E. coli*. Generally, Addition of silver to iron oxide nanoparticle increase antibacterial activity and catalytic Activity.

5.2 Recommendation

Based on the present finding, Fe_3O_4 NPs, Ag NPs and Fe_3O_4@Ag NC could be synthesized using essential oil composition of *Solanum incanum* root as a reducing agent, but the composition of aromatic plants, usually varies considerably because of both intrinsic (sexual, seasonal, ontogenetic, and genetic variations) and extrinsic (ecological and environmental aspects), to synthesize nanoparticle under this study such variation not studied, so it needs further study and comparison. Adsorption parameter such as temperature and pH are important to optimize activity of nanomaterials, but due to time and laboratory facility constraint it was not studied under this research work.

Reference

1. Hasan, S., A Review on Nanoparticles: Their Synthesis and Types. Research Journal of Recent Sciences, 2015. 4(2277-2502): p. 1-3.
2. Shanmugam, P.H.a.S., Nanoparticle Characterization and Application. International Journal Current Microbiol.App.Sci, 2015. 4: p. 379-386.
3. Chouhan, N., Silver Nanoparticles: Synthesis, Characterization and Applications, in Silver Nanoparticles - Fabrication, Characterization and Applications. 2018.
4. Álvaro de Jesús Ruíz-Baltazara, S.Y.R.-L. , and A.I.R.-C. María de Lourdes Mondragón-Sánchezc, Ramiro Pérez, Eco-friendly synthesis of Fe_3O_4 nanoparticles: Evaluation of their catalytic activity in methylene blue degradation by kinetic adsorption models. Journal of Results in Physics 2019. 12 p. 989–995.
5. Singh, P., M. Shukla, and C. Upadhyay, Signatures of consolidated superparamagnetic and spin-glass behavior in magnetite-silver core-shell nanoparticles. Nanoscale, 2018. 10(47): p. 22583-22592.
6. Altangerel Amarjargal, L.D.T., Ik-Tae Im, Cheol Sang Kim, Simultaneous preparation of Ag/Fe3O4 core–shell nanocomposites with enhanced magnetic moment and strong antibacterial and catalytic properties. Chemical Engineering Journal, 2013. 226: p. 243–254.
7. Huq, M.A., Green Synthesis of Silver Nanoparticles Using Pseudoduganella eburnea MAHUQ-39 and Their Antimicrobial Mechanisms Investigation against Drug Resistant Human PathogenInternational Journal of Molecular Sciences, 2020. 21: p. 1510.
8. Tahir Iqbal, A.H., Synthesis of Iron Oxide, Cobalt oxide and Silver Nanoparticles by Different Techniques. . International Journal of Scientific & Engineering Research, 2016. 7 (2229-5518): p. 1178- 1215.
9. Moghaddam, M. and L. Mehdizadeh, Chemistry of Essential Oils and Factors Influencing Their Constituents, in Soft Chemistry and Food Fermentation. 2017. p. 379-419.
10. Christian, P., et al., Nanoparticles: structure, properties, preparation and behaviour in environmental media. Ecotoxicology, 2008. 17(5): p. 326-43.
11. Fall, R., et al., Chemical characterization of essential oil from the leaves of Callistemon viminalis (D.R.) and Melaleuca leucadendron (Linn.). Asian Pac J Trop Biomed, 2017. 7(4): p. 347–351.

12. Ewais, E., et al., Antimicrobial Activities of Solanum Incanum, Elettaria Cardamomum and Zingiber Officinale, Used Traditionally to Treat Pathogenic Microbes. Scientific Journal of Flowers and Ornamental Plants, 2014. 1(3): p. 253-263.
13. Assefa, A., et al., Spasmolytic activity of the aqueous root extract of solanum incanum, solanaceae. Ethiop. J. Biol. Sci., 2006. 5(2): p. 137-146.
14. Zuzarte, M. and L. Salgueiro, Essential Oils Chemistry, in Bioactive Essential Oils and Cancer. 2015. p. 19-61.
15. Vidya Vilas , D.P., , Joseph Mathew Essential oil mediated synthesis of silver nanocrystals for environmental, anti-microbial and antioxidant applications Materials Science and Engineering C 2016. 61: p. 429–436.
16. Chunyan Yong, X.C., Qian Xiang, Qiang Li, Xiaodong Xing, Recyclable magnetite-silver heterodimer nanocomposites with durable antibacterial performance. Bioactive Materials 2018. 3: p. 80-86.
17. R. V. Solomon, I.S.L., J. P. Merlin, and P. Venuvanalingam, Enhanced photocatalytic degradation of azo dyes using nano Fe3O4. " Journal of the Iranian Chemical Society 2011: p. 121–128.
18. Chentao Hou , B.H.a.J.Z., Photocatalytic Degradation of Methylene Blue over TiO2 Pretreated with Varying Concentrations of NaOH. Journal of catalysts, 2018. 8: p. 575.
19. Tanih, N.F., et al., Detection of pathogenic Escherichia coli and Staphylococcus aureus from cattle and pigs slaughtered in abattoirs in Vhembe District, South Africa. ScientificWorldJournal, 2015. 2015: p. 195972.
20. Ibrahim, M.E., et al., Characterization of essential oil content isolated from Rhus flexicauli (Baker). International Food Research Journal, 2017. 24(2): p. 897-899.
21. Raut, J.S. and S.M. Karuppayil, A status review on the medicinal properties of essential oils. Industrial Crops and Products, 2014. 62 p. 250–264.
22. Hesham H. A. Rassem, Abdurahman H. Nour, and R.M. Yunus, Techniques For Extraction of Essential Oils From Plants. Australian Journal of Basic and Applied Sciences, 2016. 10(16: p. 117-127.
23. Bezerra, D.P., et al., Bioactive Essential Oils and Cancer. Moniz Research Center, Oswaldo Cruz Foundation, 2015(978-3-319-19143-0).

24. Morsy, N.F.S., Chemical Structure, Quality Indices and Bioactivity of Essential Oil Constituents, in Active Ingredients from Aromatic and Medicinal Plants. 2017.
25. Hamid, A.A., Aiyelaagbe, O.O. and Usman, L.A., Essential oils: Its medicinal and pharmacological uses. International Journal of Current Research, 2011. 3(2,): p. 086-098.
26. El Asbahani, A., et al., Essential oils: from extraction to encapsulation. Int J Pharm, 2015. 483(1-2): p. 220-43.
27. Pavlić, B., et al., Isolation of coriander (Coriandrum sativum L.) essential oil by green extractions versus traditional techniques. The Journal of Supercritical Fluids, 2015. 99: p. 23-28.
28. Masango, P., Cleaner production of essential oils by steam distillation. Journal of Cleaner Production, 2005 13: p. 833-839.
29. Maqbool, S.Z.H.a.K., GC-MS: Principle, Technique and its application in Food Science. Int j curr sci 2014. 13: p. 116-126.
30. Martinez, E.E.S.a.J.R., Identification of Essential Oil Components. 2018: p. 57-111.
31. Gatoo, M.A., et al., Physicochemical properties of nanomaterials: implication in associated toxic manifestations. Biomed Res Int, 2014. 2014: p. 498420.
32. Zhang, J.Z., Optical Properties and Spectroscopy Of Nanomaterials-WS. 2009. p. 1.
33. Coronado, E.A., Encina, E. R. ,Stefani, F. D., Optical properties of metallic nanoparticles: manipulating light, heat and forces at the nanoscale. Nanoscale, 2011. 3(10): p. 4042-59.
34. Mittal, A.K. and U.C. Banerjee, Current status and future prospects of nanobiomaterials in drug delivery, in Nanobiomaterials in Drug Delivery. 2016. p. 147-170.
35. Akbarzadeh, A., M. Samiei, and S. Davaran, Magnetic nanoparticles: preparation, physical properties, and applications in biomedicine. Nanoscale Res Lett, 2012. 7(1): p. 144.
36. Dadashi, S., R. Poursalehi, and H. Delavari, Structural and Optical Properties of Pure Iron and Iron Oxide Nanoparticles Prepared via Pulsed Nd:YAG Laser Ablation in Liquid. Procedia Materials Science, 2015. 11: p. 722-726.
37. Hayrunnisa Nadaroglu, A.A., Selvi Ince, Synthesis of Nanoparticles by Green Synthesis Method. International Journal of Innovative Research and Reviews, 2017. 1(1) p. 6-9.
38. Khan, I., K. Saeed, and I. Khan, Nanoparticles: Properties, applications and toxicities. Arabian Journal of Chemistry, 2019. 12(7): p. 908-931.

39. Yen Pin Yew, K.S., Mikio Miyake, Nurul Bahiyah Bt Ahmad Khairudin, Shaza Eva Bt Mohamad, Takeru Naiki, Kar Xin Lee, Green biosynthesis of superparamagnetic magnetite Fe3O4 nanoparticles and biomedical applications in targeted anticancer drug delivery system. Arabian Journal of Chemistry, 2020. 13: p. 2287–2308.
40. Salma Ahmed Alzahrani, M.A.M., Shaeel Ahmed Al-Thabaiti1, Zaheer Khan, Seedless synthesis and efficient recyclable catalytic activity of Ag@Fe nanocomposites towards methyl orange. Applied Nanoscience 2018. 8: p. 255–271.
41. Attarad Ali, H.Z., Synthesis, characterization, applications, and challenges of iron oxide nanoparticles. Nanotechnology, Science and Applications, 2016 9: p. 49–67.
42. Ajay Vasudeo Rane, K.K., V.K. Abitha and Sabu Thomas., Methods for Synthesis ofNanoparticles and Fabricationof Nanocomposites. 2018. 24
43. C.P. Devatha , A.K.T., Shweta Y. Katte Green synthesis of iron nanoparticles using different leaf extracts for treatment of domestic waste water. Journal of Cleaner Production 2016). 139 p. 1425-1435.
44. A. Sengottaiyan, R.M.-K.-H., Green synthesis of silver nanoparticles using Solanum indicum L. and their antibacterial. splenocyte cytotoxic potentials, 2015.
45. R.R.Thanighaiarassu, B.N.a.D.R.R., Green synthesis of silver nanoparticles and characterization using plant leaf essential oil compound citral and their antifungal activity against human pathogenic fungi. Journal of Pharmacognosy and Phytochemistry 2018 7(6): p. 902-907.
46. Dr. Ramya, B.N.a.R.T., Green fabrication of silver nanoparticles and characterization with plant leaf essential oil compound Geraniol and their antifungal activity against human pathogenic fungi. The Pharma Innovation Journal, 2018. 7(11): p. 448-453.
47. R.R. Thanighai arassu, B.N., D.R. Ramya, Green synthesis of silver nanoparticles and characterization using plant leaf essential oil rosemarinus officinalis and their antifungal activity against human pathogenic fungiJournal of Scientific Research in Pharmacy, 2018. 7(11): p. 138-144.
48. Vidya Vilas, D.P., Joseph Mathew, Essential oil mediated synthesis of silver nanocrystals for environmental, anti-microbial and antioxidant applications. Materials Science and Engineering C 2016. 61 p. 429–436.

49. Thandapani Gomathi, K.R., V. Kanchana, P. N. Sudha and K. Parthasarathy, Impact of Nanoparticle Shape, Size, and Properties of the Sustainable Nanocomposites. 2019: p. 313-336.
50. Mohaddeseh Sajjadi, M.N., S. Mohammad Sajadi, Green synthesis of Ag/Fe3O4 nanocomposite using Euphorbia peplus Linn leaf extract and evaluation of its catalytic activity. Journal of Colloid and Interface Science, 2017. 497 p. 1–13.
51. Z A Elhouderi, D.P., Synthesis, characterization, and application of Fe_3O_4 composites for mercury removal from water. 2016.
52. Tung le M, C.N., Synthesis, Characterizations of Superparamagnetic Fe_3O_4-Ag Hybrid Nanoparticles and Their Application for Highly Effective Bacteria Inactivation. . J Nanosci Nanotechnol,, . (2016). . 16(6) p. 5902-5912.
53. Carmen Chifiriuc, V.G., Alexandru Mihai Grumezescu, Crina Saviuc, Veronica Lazăr and Ecaterina Andronescu, Hybrid magnetite nanoparticles/Rosmarinus officinalis essential oil nanobiosystem with antibiofilm activity. Nanoscale Research Letters 2012. 7: p. 209.
54. Vidya Vilas, D.P., Joseph Mathew, Essential oil mediated synthesis of silver nanocrystals for environmental, anti-microbial and antioxidant applications. Materials Science and Engineering C 2016. 61: p. 429–436.
55. Ion Anghel, A.M.G., Alina Maria Holban, Anton Ficai , Alina Georgiana Anghel and Mariana Carmen Chifiriuc, Biohybrid Nanostructured Iron Oxide Nanoparticles and Satureja hortensis to Prevent Fungal Biofilm Development. International Journal of Molecular Sciences, 2013. 14: p. 18111-18122.
56. Seyed Fakhreddin Hosseinia, M.Z., Masoud Rezaeia, Farhid Farahmandghavic, Two-step method for encapsulation of oregano essential oil in chitosan nanoparticles: Preparation, characterization and in vitro release study. Carbohydrate Polymers 2013. 95: p. 50– 56.
57. Douglas D. Bannerman, M.J.P., Jai-Wei Lee, Xin Zhao, Jayne C. Hope, and Pascal Rainard, Escherichia coli and Staphylococcus aureus Elicit Differential Innate Immune Responses following Intramammary Infection. Clinical and diagnostic laboratory immunology, 2004. 11(3): p. 463–472.
58. Steven Y. C. Tong, J.S.D., Emily Eichenberger, Thomas L. Holland, Vance G. Fowler, Jr, Staphylococcus aureus Infections: Epidemiology, Pathophysiology, Clinical Manifestations, and Management. Clinical Microbiology 2015. 28 (3).

59. Maria Eugeˆnia F. Brollo, R.L.-R., Compact Ag@Fe3O4Core-shell Nanoparticles by Means of Single-stepThermal Decomposition Reaction. Scientific reports, 2014. 4: p. 6839
60. Yevgen Levitin, T.C., Obtaining of Ag@Fe Magnetic Nanocomposite With The Core-Shell Structure For Medical Purpose. Scripta Scientifica Pharmaceutical, 2015. 2(1): p. 53-59.
61. Shojaosadati, S.M.G.a.S.A., Evaluation of the antibacterial activity of Ag/Fe_3O_4 nanocomposites synthesized using starch. Carbohydrate Polymers 2016 144: p. 454–463.
62. Olena Ivashchenko, M.L., Barbara Peplińska, Marcin Jarek , Grzegorz Nowaczyk , Maciej Wiesner,Karol Załęski, Tetyana Babutina, Alicja Warowicka , Stefan Jurga Synthesis and characterization of magnetite/silver/antibiotic nanocomposites for targeted antimicrobial therapy. Materials Science and Engineering C 2015. 55: p. 343–359.
63. Sajjadi, M., M. Nasrollahzadeh, and S. Mohammad Sajadi, Green synthesis of Ag/Fe(3)O(4) nanocomposite using Euphorbia peplus Linn leaf extract and evaluation of its catalytic activity. J Colloid Interface Sci, 2017. 497: p. 1-13.
64. Amarjargal, A., et al., Simultaneous preparation of Ag/Fe_3O_4 core–shell nanocomposites with enhanced magnetic moment and strong antibacterial and catalytic properties. Chemical Engineering Journal, 2013. 226: p. 243-254.
65. Navin Jain, A.B., Jitendra Panwar, Enhanced photocatalytic degradation of methylene blue using biologically synthesized ‘‘protein-capped’’ ZnO nanoparticles. Chemical Engineering Journal 2014. 243 p. 549–555.
66. Swati Raina, A.R., Navneeta Bharadvaja, Degradation of dyes using biologically synthesized silver and copper nanoparticles. Environmental Nanotechnology, Monitoring & Management 2020 13 p. 100278.
67. J.-M. Lee, M.-S.K., and B.-W. Kim, “Photodegradation of bisphenol-A with TiO2 immobilized on the glass tubes including the UV light lamps,” Water Research, 2018. 38: p. 3605–3613.
68. Bozovic, M., et al., Esential oils extraction: a 24-hour steam distillation systematic methodology. Nat Prod Res, 2017. 31(20): p. 2387-2396.
69. Ahmed, S., et al., Green synthesis of silver nanoparticles using Azadirachta indica aqueous leaf extract. Journal of Radiation Research and Applied Sciences, 2019. 9(1): p. 1-7.

70. Yew, Y.P., et al., Green Synthesis of Magnetite (Fe3O4) Nanoparticles Using Seaweed (Kappaphycus alvarezii) Extract. Nanoscale Res Lett, 2016. 11(1): p. 276.
71. Mohaddeseh Sajjadi , M.N., S. Mohammad Sajadi Green synthesis of Ag/Fe3O4 nanocomposite using Euphorbia peplus Linn leaf extract and evaluation of its catalytic activity. Journal of Colloid and Interface Science, 2017. 497: p. 1–13.
72. J.-M. Lee, M.-S.K., and B.-W. Kim, Photodegradation of bisphenol-A with TiO2 immobilized on the glass tubes including the UV light lamps. Water Research, 2004. 38(16) p. 3605–3613.
73. Mascolo, M.C., Y. Pei, and T.A. Ring, Room Temperature Co-Precipitation Synthesis of Magnetite Nanoparticles in a Large pH Window with Different Bases. Materials (Basel), 2013. 6(12): p. 5549-5567.
74. Jemal, K., B. V. Sandeep, and S. Pola, Synthesis, Characterization, and Evaluation of the Antibacterial Activity ofAllophylus serratusLeaf and Leaf Derived Callus Extracts Mediated Silver Nanoparticles. Nan. mat., 2017. 2017: p. 1-11.
75. Fajaroh, F. and Nazriati, Factors Influence the Structural and Magnetic Properties of Ag-Fe3O4 Nanocomposites Synthesized by Reduction Method. IOP Conf. Ser.: Mater. Sci. Eng. , 2017 202(012064).
76. Aarti R. Deshmukh, A.G., and Beom SooKim, Ultrasound Assisted Green Synthesis of Silver and Iron Oxide Nanoparticles Using Fenugreek Seed Extract and Their Enhanced Antibacterial and Antioxidant Activities. BioMed Research International, 2019. 2019: p. 14.
77. Bhupendra Chudasama, A.K.V., Nidhi Andhariya , R.V. Upadhyay , R.V. Mehta, Antifungal activity of multifunctional Fe3O4–Ag nanocolloids. Journal of Magnetism and Magnetic Materials, 2011. 323: p. 1233–1237.
78. Movasaghi, Z., S. Rehman, and D.I. ur Rehman, Fourier Transform Infrared (FTIR) Spectroscopy of Biological Tissues. Applied Spectroscopy Reviews, 2008. 43(2): p. 134-179.
79. prem, V.k.v.g.a.a.a., Green Synthesis and Characterization of Iron Oxide Nanoparticles Using Phyllanthus Niruri Extract. Oriental journal of chemistry, 2018. 2583-2589: p. 34(5).

80. Wensheng Lu , Y.S., Anjian Xie, Weiqiang Zhang Green synthesis and characterization of superparamagnetic Fe3O4 nanoparticles. Journal of Magnetism and Magnetic Materials, 2010. 322 p. 1828–1833.
81. Loh, K.-S., et al., Use of Fe3O4 Nanoparticles for Enhancement of Biosensor Response to the Herbicide 2,4-Dichlorophenoxyacetic Acid. Sensors, 2008. 8(9): p. 5775-5791.
82. Ivashchenko, O., et al., Synthesis and characterization of magnetite/silver/antibiotic nanocomposites for targeted antimicrobial therapy. Materials Science and Engineering C, 2015. 55: p. 343–359.
83. K. Anandalakshmi , J. Venugoba, and V. Ramasamy, Characterization of silver nanoparticles by green synthesis method using Pedalium murex leaf extract and their antibacterial activity. App Na sci, 2015. 6(3): p. 399-408.
84. Viju Kumar V G and A.A. Prem, Green Synthesis and Characterization of Iron Oxide Nanoparticles Using Phyllanthus Niruri Extract. Oriental Journal of Chemistry, 2018. 34(5): p. 2583-2589.
85. Hesham Fouad Aly, A.I.A.-E., Photocatalytic Degradation of Methylene Blue Dye Using Silica Oxide Nanoparticles as a Catalyst. Water Environ. Res., 2018. 90: p. 807
86. A. M. Asiri, M.S.A.-A., T. A. Al-Talhi, and A. D. Al-Talhi Photodegradation of Rhodamine 6G and phenol red by nanosized TiO_2 under solar irradiation. Journal of Saudi Chemical Society, 2011. 15(2): p. 121–128.
87. R. V. Solomon, I.S.L., J. P. Merlin, and P. Venuvanalingam, Enhanced photocatalytic degradation of azo dyes using nano Fe_3O_4. Journal of the Iranian Chemical Society, 2012. 9(2): p. 101–109, .
88. Y. Yao, Y.C., F. Lu, F. Wei, X. Wang, and S. Wang, Magnetic recoverable $MnFe_2O_4$ and $MnFe_2O_4$-graphene hybrid as heterogeneous catalysts of peroxymonosulfate activation for efficient degradation of aqueous organic pollutants. Journal of Hazardous Materials, 2014. 270: p. 61–70.
89. Raid A. Ismail , G.M.S., Safa A. Abdulrahman, Thorria R. Marzoog, Antibacterial activity ofmagnetic iron oxide nanoparticles synthesized by laser ablation in liquid. Materials Science and Engineering C, 2015. 53: p. 286–297.